Title: The glymphatic system clears amyloid beta and tau from brain to plasma in humans

Authors: Paul Dagum, MD, PhD[1]; Donald L. Elbert, PhD[2]; Laurent Giovangrandi, PhD[1]; Tarandeep Singh, MS[1]; Venky V. Venkatesh, PhD, PMP[3]; Alejandro Corbellini, PhD[1]; Robert M. Kaplan, PhD[4]; Swati Rane Levendovszky, PhD[5,6] ; Elizabeth Ludington[7], PhD; Kevin Yarasheski, PhD[3]; Jeffrey Lowenkron[8], MD, MPP; Carla VandeWeerd, PhD[9,10]; Miranda M. Lim, MD, PhD[11,12,13]; Jeffrey J. Iliff, PhD[2,14,15]

Affiliations: [1]Applied Cognition Inc., Redwood City CA; [2]Department of Neurology, University of Washington School of Medicine, Seattle WA; [3]C_2N Diagnostics, St. Louis, MO; [4]Clinical Excellence Research Center, Stanford University School of Medicine, Stanford, CA; [5]Department of Radiology, University of Washington School of Medicine, Seattle, WA; [6]Department of Radiology, Kansas University Medical Center, Kansas City KS; [7]Epalla Consulting, San Diego, CA; [8]The Villages Health System, The Villages, FL; [9]University of Florida Precision Health Research Center, University of Florida, Gainesville, FL; [10]Health Outcomes and Biomedical Informatics, College of Medicine, University of Florida, Gainesville, FL; [11]VISN 20 Northwest Mental Illness Research, Education and Clinical Center (MIRECC), VA Portland Health Care System, Portland, OR; [12]Neurology Service, Research Service, VA Portland Health Care System, Portland, OR; [13]Department of Neurology, Oregon Alzheimer's Disease Research Center, Oregon Health & Science University, Portland, OR; [14]VISN 20 Northwest Mental Illness Research, Education and Clinical Center, VA Puget Sound Healthcare System, Seattle WA; [15]Department of Psychiatry and Behavioral Sciences;

Corresponding Author:
Paul Dagum, MD PhD
Applied Cognition Inc
1629 Main St.
Redwood City, CA 94063
paul@appliedcognition.com
Ph: (415) 378-5456

ABSTRACT

Poor sleep is implicated in the development of Alzheimer's disease (AD) pathology and cognitive impairment. Dysfunction of the glymphatic system has been proposed as a mechanistic link between sleep disruption and AD, and in animal models glymphatic impairment is sufficient to drive the development of AD pathology. It remains unknown whether the glymphatic system clears amyloid beta (Aβ) and tau from the brain in humans. This study directly tested the hypothesis that sleep-active glymphatic clearance increases morning plasma AD biomarker levels. In a multi-site randomized crossover clinical trial, participants (N=39) underwent overnight in-laboratory conditions of normal sleep and sleep deprivation following instrumentation that included a novel device to measure sleep features by electroencephalography (EEG), cerebrovascular compliance by measurement of pulse transit time (PTT), and brain parenchymal resistance to glymphatic flow (R_P) by transcranial multifrequency impedance spectroscopy. We evaluated whether R_P, sleep EEG features, PTT, and heart rate variability (HRV) predicted overnight changes in plasma AD biomarker (Aβ40, Aβ42, np-tau181, np-tau217 and p-tau181) levels. We found that changes in R_P, PTT, HRV and EEG delta power in a multivariate linear mixed model predicted sleep-associated overnight changes in Aβ40 ($p=0.013$), Aβ42 ($p<0.001$), np-tau181 ($p<0.001$), np-tau217 ($p<0.001$) and p-tau181 ($p<0.001$). The predicted changes replicated those from a multicompartment model based on published data on synaptic-metabolic release and clearance of Aβ and tau to the plasma. Sensitivity analysis demonstrated that while morning biomarker levels were altered by both the synaptic-metabolic release and clearance of Aβ and tau, during sleep glymphatic clearance was the dominant influence. In contrast, during sleep deprivation (waking) while glymphatic clearance was a contributor, Aβ and tau release was the dominant factor explaining variance in morning plasma Aβ and tau levels. Our findings show that elements of sleep-active physiology, in particular decreased brain parenchymal resistance,

facilitates the overnight clearance of AD biomarkers to plasma, supporting a role for glymphatic clearance in these processes, and suggesting the enhancement of glymphatic function as a therapeutic target to reduce the development and progression of AD pathology in at-risk populations.

KEYWORDS

glymphatic, sleep, Alzheimer's, amyloid beta, tau, plasma, clearance, release, production

63 **INTRODUCTION**

64 Sleep disruption is associated with increased risk of Alzheimer's disease (AD) in
65 epidemiological studies[1-3], while biomarker studies in cognitively-intact participants suggest that
66 short sleep duration and poor sleep quality are associated with greater AD-related amyloid β
67 (Aβ) and tau pathology[4-9], even before the onset of clinical symptoms of cognitive and functional
68 decline. Yet the mechanistic link between sleep disruption and AD risk remains undefined. The
69 glymphatic system is a brain-wide network of perivascular pathways along which cerebrospinal
70 fluid (CSF) and interstitial fluid (ISF) exchange, supporting the clearance of interstitial solutes
71 from the brain into the CSF, and thence into the blood. Studies in mice demonstrated that
72 glymphatic function contributes to the clearance of Aβ and tau, is more rapid during sleep, and
73 is impaired by acute sleep deprivation[10-15]. While more rapid glymphatic clearance of solutes
74 during sleep has now been validated in the human brain[16,17], no study has tested
75 mechanistically whether sleep-active glymphatic activity contributes to the clearance of Aβ and
76 tau in a healthy human population.

77

78 Plasma biomarkers have emerged as a potentially critical tool enabling the non-invasive
79 diagnosis of AD at a large scale within the wider population. Immuno-assay and mass
80 spectrometry-based measures of different Aβ and tau species permit the assessment of AD-
81 related Aβ plaque burden and tau pathology, even during preclinical stages of disease in the
82 years prior to patients' clinical progression to cognitive impairment and dementia[18,19]. Although
83 generally regarded as steady-state indicators of brain AD pathological burden, plasma AD
84 biomarker levels are impacted acutely by sleep disruption[4,20]. While it is possible that these
85 effects reflect reduced rates of cellular Aβ and tau release during sleep, they may also reflect
86 the role of sleep-active glymphatic clearance in the transport of Aβ and tau from the brain to the
87 blood. In a crossover study including 5 healthy participants, plasma $A\beta_{40}$, $A\beta_{42}$, non-

88 phosphorylated tau181 (np-tau181), non-phosphorylated tau217 (np-tau217) and
89 phosphorylated tau181 (p-tau181) were each reduced during the overnight period by acute
90 sleep deprivation[4]. Noting an increased ratio of CSF:plasma Aβ and tau levels, the authors
91 inferred that the processes governing the clearance of Aβ and tau from the brain to the CSF,
92 and thence from the CSF to the plasma must be impaired by acute sleep deprivation. These
93 findings are consistent with the sleep-active glymphatic clearance of Aβ and tau from the brain,
94 yet they do not provide causal support. A second study showed that plasma Aβ and tau levels
95 were reduced in participants that exhibited MRI evidence of impaired glymphatic and CSF-to-
96 plasma clearance[21]. These findings established a correlation between steady-state AD
97 biomarker plasma levels and impaired CSF circulation, but did not test whether sleep-active
98 glymphatic function directly contributes to the clearance of these peptides during sleep in
99 otherwise healthy individuals.
100
101 Here we designed a study to directly test if sleep-active glymphatic function contributes to the
102 overnight clearance of Aβ and tau from the human brain. We first developed a compartmental
103 pharmacokinetic model to predict the effect that sleep-associated changes in Aβ and tau
104 release and sleep-active glymphatic clearance, reflected by transport between the brain ISF and
105 CSF, would have on morning plasma levels of Aβ and tau species. We then carried out a clinical
106 randomized crossover study where participants underwent overnight normal sleep and sleep
107 deprivation. Prior studies in rodents and humans demonstrate that glymphatic function
108 increases with increasing sleep electroencephalography (EEG) delta and theta power, reduced
109 EEG beta power, reduced heart rate (HR), reduced central noradrenergic tone, and reduced
110 brain parenchymal resistance to fluid flow (R_P), and vasomotor oscillations[13,22-26]. Measuring
111 these key determinants of glymphatic exchange with a novel investigational device[17], we
112 defined the relationship between sleep features measured by EEG, R_P measured by dynamic

113 impedance spectroscopy, and HRV and cerebrovascular compliance measured by impedance
114 plethysmography (IPG) and overnight changes in plasma AD biomarker levels. Using this
115 approach, we directly tested the hypothesis that sleep-active glymphatic clearance elevates
116 morning plasma AD biomarker levels, despite a sleep-associated reduction in their production.
117

118 **RESULTS**

119 Statistical significance tests presented in the results have not been adjusted for multiple
120 comparisons.

121 *Compartmental pharmacokinetic model relating glymphatic exchange to plasma AD biomarker*
122 *levels*

123 We first developed a compartmental pharmacokinetic model to define the effects that sleep-
124 related changes in interstitial solute release and clearance would have on overnight changes in
125 plasma levels of Aβ and tau. The model (shown in **Figure 1A**) is a simplification of prior
126 models[27] and includes the minimal number of compartments, transport and elimination
127 pathways needed to define the effect that a change in overnight interstitial solute
128 production/release and glymphatic clearance between the ISF and CSF would have on plasma
129 Aβ and tau levels. The model included a 16-hour period of wake, and either an 8-hour period of
130 sleep or an 8-hour period of sleep deprivation. It includes 6 compartments: Cellular Site of
131 Production/Release (**1**), Free ISF (**2**), CSF (**3**), Plasma (**4**), Cellular Site of Uptake/Degradation
132 (**5**), and Non-Monomeric Pools (**6**). Solute transport processes and their rate constants for Aβ
133 and tau species based on literature values[27,28] are provided in **Table 1**.
134

135 The 24-hour cellular synthesis of amyloid precursor protein (APP) and tau is invariant to sleep-
136 wake state and was modeled at a constant rate of 10 arbitrary units (a.u.) per hour[29,30]. Release
137 of cellular Aβ and tau species into the ISF in the model is controlled by the cellular solute

138 release rate constant k_{cell_rel} (**Table 1**) and was kept constant during the 16 hours of wake.
139 During the 8 hours of sleep, k_{cell_rel} was reduced by 30% consistent with reported 30% sleep
140 reduction in ISF Aβ and tau species[29,30], and during the 8 hours of sleep deprivation it was
141 reduced by 10% reflecting a circadian time-of-day effect.
142
143 This model was evaluated under two conditions. In the **null model**, sleep-active glymphatic
144 exchange was posited to not occur; therefore solute transport between the Free ISF
145 compartment (**2**) and the CSF compartment (**3**), reflected by the rate constants k_{glymph_out} and
146 k_{glymph_in}, were held constant across both sleep and waking (or sleep deprivation) states. In
147 this model, sleep-related changes in synaptic and metabolic activity, which impact cellular solute
148 release, were not permitted to vary beyond the defined reduction in the cellular solute release
149 rate constant k_{cell_rel} during the 8-hour sleep period. In the **neuro-glymphatic model**,
150 k_{glymph_out} and k_{glymph_in} increased during sleep, reflecting the sleep-active CSF solute influx
151 and interstitial solute efflux observed in both rodents and humans[13,16,17]. Additionally, k_{cell_rel}
152 either increased or decreased with sleep, representing corresponding changes in synaptic and
153 metabolic activity that affect solute release into the brain interstitium[30,31].
154
155 The full derivation of the compartmental pharmacokinetic model is provided in **Supplementary**
156 **Methods and Results. Figure 1B** presents the steady-state compartmental concentrations of
157 Aβ and tau over a 48-hour period under the **null model** (solid lines), as well as under **neuro-**
158 **glymphatic model** scenarios involving increased glymphatic clearance (dashed lines) and
159 elevated synaptic-metabolic release (dotted lines). **Figure 1C** illustrates alternative **neuro-**
160 **glymphatic model** scenarios with reduced glymphatic clearance (dashed lines) and decreased
161 synaptic-metabolic release (dotted lines), shown in comparison to the **null model** (solid lines).
162 Across all scenarios, both Aβ and tau concentrations in the plasma increase or decrease

relative to the **null model**, depending on whether glymphatic clearance or synaptic-metabolic release is enhanced or diminished, respectively, over the 48-hour period. These plots demonstrate that changes in Aβ and tau concentrations within the plasma and CSF compartments cannot independently distinguish between decreased glymphatic clearance and decreased solute release, nor between increased glymphatic clearance and increased solute release. An additional derivation of the model, described in detail in the **Supplementary Methods and Results**, demonstrates that within the in the **null model,** morning plasma levels will be linearly dependent on evening plasma levels only, whereas the **neuro-glymphatic model** has a contribution from the interaction term between the evening plasma levels and the variable rate constants k_{glymph_out}, k_{glymph_in} and k_{cell_rel}.

We next compared changes in plasma levels of species that remained primarily monomeric in form (Aβ40, np-tau), and species that are prone to form non-monomeric aggregates (Aβ42, p-tau) following increases and decreases in glymphatic clearance and synaptic-metabolic release. If this tendency to form aggregates is ignored, and rate constants for monomer-to-aggregate conversion is set to zero ($k_{on-rate} = 0$), changes in cellular release k_{cell_rel} or clearance k_{glymph_out} have no effect on the Aβ42/Aβ40 or p-tau/np-tau ratios (**Supplemental Table 1**, top row). In contrast, when the tendency for Aβ42 and p-tau to form non-monomeric aggregates is included in the model ($k_{on-rate} > 0$), increased and decreased solute release and glymphatic clearance shift plasma Aβ42/Aβ40 or p-tau/np-tau ratios (**Supplemental Table 1**). Both the Aβ42/Aβ40 or p-tau/np-tau ratios increase in response to decreased production or increased glymphatic clearance, and decrease in response to increased production or reduced clearance. This suggests that non-monomeric aggregates act both as a secondary source of monomeric Aβ42 and p-tau species under conditions of reduced production and as an additional sink for these species under conditions of reduced clearance. Under conditions of increased glymphatic

188 clearance, the enhanced removal of Aβ42 and p-tau from the ISF reduces their opportunity to
189 aggregate, resulting in a higher proportion reaching the plasma relative to Aβ40 and np-tau—
190 thus increasing their respective plasma ratios. Taken together, this suggests that changes in
191 plasma Aβ42/Aβ40 or p-tau/np-tau ratios allow us to infer the predominant mechanism driving
192 changes in morning plasma AD biomarker levels under sleep or sleep-deprivation conditions in
193 experimental settings.
194
195 These pharmacokinetic modeling results provide three concrete predictions that permit us to
196 test the hypothesis that sleep-active glymphatic exchange contributes to overnight changes in
197 plasma AD biomarker levels independent of sleep-dependent changes in solute release:
198
199 **1)** Under the **neuro-glymphatic model**, compared to normal sleep, decreased clearance
200 during overnight sleep deprivation would reduce morning plasma AD biomarker levels
201 while increased production would increase levels.
202
203 **2)** Under the **neuro-glymphatic model**, under conditions of sleep deprivation, morning
204 plasma AD biomarker levels would increase by the interaction term between evening
205 plasma levels and features of synaptic-metabolic activity contributing to greater
206 production; under normal sleep conditions morning plasma AD biomarker levels will be
207 increased by the interaction term between evening plasma levels and features of sleep-
208 active glymphatic function contributing to greater clearance.
209
210 **3)** Under the **neuro-glymphatic model**, under normal sleep conditions morning plasma
211 Aβ42/Aβ40 and p-tau/np-tau ratios will increase with greater sleep-dependent clearance;
212 overnight sleep deprivation will decrease these ratios from greater wake-dependent
213 production.

214

215 *Clinical study design and participant demographic data*

216 As described previously[17], we conducted two cross-over clinical studies in which participants
217 underwent one night of normal sleep and one night of sleep deprivation, in randomized order
218 and separated by two or more weeks (**Figure 2A**). One study was conducted in The Villages®
219 community in Central Florida where the University of Florida maintains a satellite academic
220 research center, The UF Health Precision Health Research Center (UF Health PHRC). The
221 second study was carried out at the University of Washington (UW) in Seattle. Study
222 participants underwent peripheral blood draws at 1900 hrs and 0700 hrs, prior to and following
223 the overnight sleep and sleep deprivation periods. Plasma AD biomarkers, including $A\beta_{40}$, $A\beta_{42}$,
224 np-tau181, np-tau217, p-tau181, and phosphorylated tau217 (p-tau217) were quantified using
225 C_2N Diagnostics' immunoprecipitation liquid chromatography-tandem mass spectrometry
226 platforms[32-34]. Details of specimen collection and processing are provided in **Supplementary**
227 **Methods and Results.** During the overnight period, participants were instrumented with an
228 investigational in-ear wearable device that measured key determinants of glymphatic function,
229 including sleep features (hypnogram and spectral band power) by electroencephalography
230 (EEG), heart rate variability (HRV) by photoplethysmography (PPG), cerebrovascular pulse
231 transit time (PTT) by impedance plethysmography (IPG), and brain parenchymal resistance (R_P)
232 by dynamic impedance spectroscopy (**Figure 2B**). A detailed description of this device, the
233 validation of its sleep EEG measures against gold-standard overnight polysomnography, and of
234 the measures of R_P against contrast-enhanced magnetic resonance imaging (CE-MRI)-based
235 measures of glymphatic function has recently been reported[17]. Cerebrovascular PTT
236 measurements obtained using impedance plethysmography were validated against contrast-
237 enhanced MRI-based measures of cerebrovascular function, as detailed in the **Supplemental**
238 **Methods and Results (Supplemental Tables 2 – 6)**.

239

240 All studies were performed between October 2022 – June 2023 and were reviewed and
241 approved by University of Florida Institutional Review Board (IRB No. 202201364, Villages
242 study) and Western Institutional Review Board (IRB No. 20225818, UW study). The studies
243 have been registered at ClinicalTrials.gov (https://clinicaltrials.gov/study/NCT06060054 and
244 https://clinicaltrials.gov/study/NCT06222385). Written informed consent was obtained from all
245 study participants during a screening visit, prior to any study activities. Studies were carried out
246 in accordance with the principles of the Belmont Report. The Villages Study enrolled 34 healthy
247 participants 56-66 years of age. The UW Study enrolled 14 healthy participants 49-63 years of
248 age. Participants were excluded if they had cognitive impairment or clinical depression.
249 Cognitive impairment was assessed using the Montreal Cognitive Assessment (MoCA, 28.1 +/-
250 1.2; range 26, 30) and depression was evaluated using the 15-item Geriatric Depression Scale
251 (GDS, 0.7 +/- 1.2; range 0, 4). Participants with a self-reported history of diabetes, hypertension,
252 coronary artery disease, pulmonary disease, neurological disease, depression, or anxiety were
253 excluded from the study. Exclusion also applied to participants planning travel to alternate time
254 zones within two weeks of study participation, as well as those with a formal diagnosis of any
255 sleep disorder (e.g., sleep apnea requiring positive airway pressure [PAP] therapy, insomnia,
256 restless leg syndrome, circadian rhythm sleep disorder, or parasomnia). To minimize
257 preparation bias (i.e., altering sleep schedules or taking naps in anticipation of sleep deprivation
258 visits), participants were not informed of their initial visit assignment until 4:00 PM on the day of
259 arrival. Sleep quality prior to and between study visits was subjectively evaluated based on
260 investigator assessment. Participant demographics, MoCA and GDS scores are listed for each
261 study site and for the combined dataset in **Table 2**.
262
263 A Consolidated Standards of Reporting Trials (CONSORT) diagram for the Villages Study and
264 UW Study is provided in **Figure 2C.** Within the Villages Study, the first three participants were
265 removed from analysis because of a sensor position change in the investigational device. One

266 participant was unable to complete the first MRI session and withdrew from the study. Of the
267 remaining 30 participants (61.8 ± 2.7 years of age; 14 female, 16 male) that completed the
268 Villages Study, five overnight sleep studies and eight overnight wake studies failed data quality
269 control due to excessive artifacts in the recordings, leaving 25 sleep studies and 22 wake
270 studies with analyzable device and biomarker data in the Villages Study. Of the participants
271 enrolled in the UW Study, one was not compliant with the enforced wake protocol and was
272 removed from analysis. A second participant was also excluded because of missing EEG
273 powerband data during REM sleep caused by artifacts, which was required for the current
274 analysis. The remaining 13 participants (55.9 ± 4.6 years of age; 6 female, 7 male) all
275 completed the protocol. All overnight sleep data were usable, but two overnight wake studies
276 were removed because of excessive artifact in the UW Study.
277
278 We measured plasma $A\beta_{40}$, $A\beta_{42}$, np-tau181, np-tau217, p-tau181, and p-tau217 at evening and
279 morning timepoints in each participant prior to and following overnight sleep or sleep
280 deprivation. Summary plasma AD biomarker levels are provided in **Table 3**. Of 38 participants,
281 a total of 11 were assessed as 'amyloid-positive' by the C2N mass spectrometry with a $A\beta_{42}$/
282 $A\beta_{40}$ cutoff value of 0.089[32,34,35] (**Table 2**). Plasma AD biomarker levels shown in **Table 3** are
283 stratified by participant amyloid status. Overall, the measured plasma levels and overnight
284 changes with sleep agree with prior reported *values* for $A\beta_{40}$, $A\beta_{42}$ and p-tau181[36]. Furthermore,
285 the overnight changes in measured plasma levels following sleep and sleep-deprivation did not
286 differ significantly, consistent with the possibility of competing clearance or production effects
287 during sleep and sleep-deprivation.
288
289 We further investigated potential sequence-related effects within the randomized cross-over
290 study design by comparing the evening-minus-morning plasma biomarker levels following sleep

291 and/or sleep deprivation on the first visit with those on the second visit. This analysis was
292 conducted separately for amyloid-positive and amyloid-negative groups, as well as for the
293 combined amyloid positive and negative cohorts. A total of 40 distinct comparisons were made.
294 Only two showed significant sequence differences between the first and second visits: (i) in the
295 amyloid-negative group under sleep deprivation, **np-tau217** showed a difference (P = 0.031); (ii)
296 in the combined amyloid group under sleep deprivation, **np-tau181** showed a difference (P =
297 0.043).
298
299 *Development of a multivariate model to relate release and glymphatic clearance features to*
300 *plasma Aβ and tau concentrations*
301 We developed a series of multivariate mixed models to define the effects that continuous
302 features of glymphatic physiology and synaptic-metabolic activity have on overnight release and
303 clearance of brain interstitial Aβ and tau to the plasma. Within these models, the multiple
304 dependent variable measures for each participant were the morning plasma Aβ and tau
305 (Aβ40, Aβ42, np-tau181, np-tau217, p-tau181) biomarker levels. Plasma p-tau217 levels were
306 measured but excluded from analysis because a large proportion (9 out of 49) of these
307 cognitively-intact individuals exhibited plasma p-tau217 levels below the limit of detection for the
308 assay, consistent with prior study findings[37,38]. Data from amyloid-negative and amyloid-positive
309 individuals were analyzed separately.
310
311 Because of the large number of measured outcomes, we used dimensionality reducing single-
312 index regression[39] to combine sleep-related factors into single 'predictors'. A detailed
313 explanation of this single predictor development is provided in **Supplementary Methods and**
314 **Results.** Within these models, two distinct groups of predictors were analyzed:
315 neurophysiological variables (***Physio***) and hypnographic sleep stages (***Hypno***). Separating

316 predictors into these groups enabled comparison of both neurophysiological measures and
317 sleep stage durations in explaining observed differences in morning plasma Aβ and tau levels,
318 while mitigating multicollinearity among EEG power bands and sleep stages in the regression
319 models, as previously documented[17]. The first group of predictors (***Physio***) included EEG non-
320 rapid eye movement (NREM) delta (0.5–4 Hz) and theta power bands, REM sleep theta and
321 beta power bands, heart rate variability (HRV), and pulse transit time (PTT) during NREM, and
322 parenchymal resistance R_P. HRV and PTT values during REM sleep were highly correlated with
323 those during NREM and were excluded. The NREM and REM power bands selected represent
324 the majority of the spectral power during these sleep stages, thus contributing to synaptic–
325 metabolic release[30,31], and because EEG delta, beta and theta power bands have established
326 associations with glymphatic clearance[13,17,22,23]. The second group (***Hypno***) comprised
327 hypnographic sleep stages, including the durations of REM, N1, NREM (N2 + N3), and wake
328 after sleep onset (WASO). Each group of individual predictors was combined using linear
329 combinations into three single-index predictors for amyloid-negative and amyloid-positive
330 participants separately: the neurophysiological predictor under the sleeping condition ($\boldsymbol{Physio_S}$)
331 and under the sleep deprivation/wake condition ($\boldsymbol{Physio_W}$), and the sleep hypnogram predictor
332 under the sleeping condition ($\boldsymbol{Hypno_S}$). The optimal predictor components and weights for the
333 sleep condition ($\boldsymbol{Physio_S, Hypno_S}$) and sleep deprivation/wake condition ($\boldsymbol{Physio_W}$), where the
334 sum of the squared weights normalizes to unity, are provided in **Table 4.**
335
336 We developed parallel multivariate linear mixed models representing the **null model** and the
337 **neuro-glymphatic model**, as described in detail in **Supplemental Methods and Results.**
338 Under the **null model**, morning plasma levels of Aβ and tau species were not dependent upon
339 sleep-active glymphatic exchange and synaptic-metabolic release, and thus were not assumed
340 to be influenced by sleep neurophysiological (***Physio***) and sleep stage (***Hypno***) predictors.
341 Rather the morning plasma levels of AD biomarkers ($\boldsymbol{Conc_{AM}}$) were regressed on the evening

342 plasma levels (***Conc$_{PM}$***) for Aβ and tau biomarkers, separately for amyloid positive and amyloid
343 negative participants. Potentially confounding variables age, sex, APOE-ε4 status, and study
344 site were included in the model. A circadian confounder was also included in the model,
345 reflecting the interval between the evening AD biomarker sample time and sleep-onset
346 measured by EEG. Multivariate mixed models used participant ID as a random intercept and the
347 categorical *biomarker* variable as a vector of random slopes. The **neuro-glymphatic model**
348 shares the features of the **null model** but included the effects of the single index predictors
349 (***Physio$_S$***, ***Physio$_W$*** or ***Hypno$_S$***), and their respective interaction terms with evening levels of
350 plasma AD biomarkers (***Physio$_S$ * Conc$_{PM}$***, ***Hypno$_S$ * Conc$_{PM}$***, ***Physio$_W$ * Conc$_{PM}$***). The
351 likelihood ratio test (LRT) of the **neuro-glymphatic model** versus the **null model** was used to
352 determine which model performed better at predicting the morning plasma Aβ and tau
353 biomarker levels. The conditional variances of each model, i.e. the residual variation *conditional*
354 *on* a participant's random effects, were used to define the amount of variance in morning
355 plasma Aβ and tau levels explained by the **neuro-glymphatic model** over that explained by the
356 **null model**. This is described in detail in **Supplementary Methods and Results.**
357
358 *Effects of sleep-related neurophysiological features on overnight Aβ and tau release and*
359 *clearance*
360 The predictor ***Physio$_S$*** that led to the best fit of the data based on maximum likelihood for the
361 **neuro-glymphatic model** in sleep for both amyloid-negative and -positive individuals showed
362 that R_P was the overwhelming contributor to ***Physio$_S$*** (**Table 4**). The output of the **null model**
363 and **neuro-glymphatic model** with the predictor ***Physio$_S$*** for both amyloid-positive and
364 amyloid-negative individuals are shown in **Table 5**. Estimates for single predictor coefficients
365 within the **neuro-glymphatic model** for each plasma AD biomarker, evaluated at the mean
366 evening biomarker level, are provided in **Supplemental Table 7**.

367

368 Within the **null model**, evening plasma Aβ and tau levels (***$Conc_{PM}$***) were the main predictor of
369 morning plasma levels in both amyloid-positive and -negative participants, reflecting between-
370 participant evening consistency in AD biomarker levels (**Table 5**). Within the **neuro-glymphatic**
371 **model**, in addition to evening plasma biomarker levels, participant age, sex, and circadian
372 alignment each significantly contributed to morning plasma Aβ and tau levels in both amyloid-
373 positive and -negative participants. APOE-e4 status was significantly associated with lower
374 morning AD biomarker levels in amyloid-positive, but not amyloid-negative individuals. Age was
375 significantly associated with higher morning AD biomarker levels in both groups. Across both
376 amyloid-positive and -negative participants, the ***$Physio_S$*** predictor significantly impacted plasma
377 Aβ and tau levels, and the ***$Conc_{PM}$**$Physio_S$*** interaction terms were consistently significant
378 across Aβ and tau analytes (**Table 5**).

379

380 By including overnight R_P, PTT, HRV, and EEG power bands in the single predictor ***$Physio_S$***,
381 the **neuro-glymphatic model** led to greater predictive performance over the **null model** (**Table**
382 **6**, LRT, $p < 0.001$). When comparing the percent variance of morning plasma AD biomarker
383 levels explained by the **neuro-glymphatic model** compared to the **null model**, inclusion of
384 overnight ***$Physio_S$*** in the **neuro-glymphatic model** explained between 49.1% (Aβ40) to 56.0%
385 (Aβ42) additional variance in amyloid-positive individuals, and between 71.3% (p-tau181) to
386 97.8% (Aβ40) in amyloid-negative individuals (**Table 7**).

387

388 As detailed above, the ***$Physio_S$*** single-index predictor includes several sleep-related
389 physiological features that could contribute variously to changes in glymphatic clearance to the
390 plasma, or to synaptic-metabolic release of Aβ and tau. We carried out a sensitivity analysis to
391 explore the relative contributions of these individual neurophysiological predictors, and of

392 glymphatic clearance versus synaptic-metabolic release to changes in morning plasma Aβ and
393 tau analyte levels. This sensitivity analysis is provided in detail in **Supplementary Methods and**
394 **Results**. The analysis suggests that parenchymal resistance R_P, cerebrovascular compliance
395 (measured by PTT) and NREM EEG delta power during sleep, which are each associated with
396 enhanced glymphatic exchange in rodents and humans[12,13,17,22,23,25,40,41], facilitated the overnight
397 clearance of brain interstitial Aβ and tau into the plasma made the largest contribution to
398 changes in plasma Aβ and tau levels. Relative to the contributions of these individual predictors,
399 the contribution from increased synaptic-metabolic activity reflected in NREM EEG theta power
400 and REM EEG theta and beta power were comparatively minor (**Supplementary Table 3**). The
401 combined effects of these predictors which impact both glymphatic clearance and synaptic-
402 metabolic release of Aβ and tau accounted for over 50% of the variance in morning plasma Aβ
403 and tau levels in amyloid-positive individuals, and over 90% of the variance in amyloid-negative
404 individuals, compared to that explained by the **null model** alone (**Table 7**). These data suggest
405 that both increased synaptic-metabolic release and glymphatic clearance of Aβ and tau during
406 sleep contribute to increased morning plasma AD biomarker levels, but that increased clearance
407 driven by reduced R_P, increased cerebrovascular compliance, and increased EEG delta power
408 are the greatest contributors to these effects.
409
410 *NREM sleep duration enhanced overnight clearance of Aβ and tau to the plasma*
411 We next tested whether differences in overnight sleep stages influenced the glymphatic
412 clearance or synaptic-metabolic release of Aβ and tau to the plasma. The predictor ***Hypno$_S$*** was
413 constructed from regressors chosen from EEG hypnogram stages REM, N1, NREM (N2, N3)
414 and WASO that led to the best fit of the data based on the maximum likelihood optimization for
415 the **neuro-glymphatic model** for amyloid-positive and amyloid-negative individuals (**Table 4**).
416 The **null model** and the **neuro-glymphatic model** fitted to the morning plasma AD biomarker

417 level data following overnight sleep with the ***Hypno$_S$*** predictor are shown in **Supplemental**
418 **Table 10**. By including overnight REM, NREM, N1 and WASO in the single predictor ***Hypno$_S$***,
419 the **neuro-glymphatic model** led to greater predictive performance over the **null model** (**Table**
420 **6**, LRT, $p < 0.001$). When comparing the percent variance of morning plasma AD biomarker
421 levels that was explained by overnight sleep stage durations in the **neuro-glymphatic model**
422 and that was not explained by the **null model**, the **neuro-glymphatic model** in amyloid-positive
423 individuals explained between 38% (all tau species) to 62.5% (Aβ42) of the variance (**Table 7**).
424 In amyloid-negative individuals, sleep stage duration did not perform better than the **null model**
425 in explaining Aβ40 and Aβ42 levels, but explained between 64% (p-tau181) and 93.1% (np-
426 tau217) of the tau variance (**Table 7**).
427
428 Using a similar approach to that above, we observed that at a mean value of each evening
429 plasma AD biomarker level, a decrease in overnight ***Hypno$_s$***, which corresponds to an increase
430 in NREM sleep duration and a decrease in REM sleep, N1 sleep, and WASO duration (**Table**
431 **4**), increases morning plasma Aβ and tau biomarker levels (**Supplemental Table 7**). Sensitivity
432 analysis, as described in **Supplementary Methods and Results** (**Supplementary Table 3-4**),
433 suggests that increased NREM sleep duration, which is associated with increased glymphatic
434 function in rodents and humans[13,16,17], increases the clearance of Aβ and tau to the plasma. A
435 decrease REM sleep, N1 sleep and WASO duration were also associated with an increase in
436 glymphatic clearance (**Supplementary Table 3**), primarily because of their negative correlation
437 with NREM sleep duration. These effects explain approximately 50% of the unexplained
438 variance in the morning plasma AD biomarker levels from the **null model** in amyloid-positive
439 individuals but fail to explain additional Aβ40 and Aβ42 variance in amyloid-negative individuals
440 (**Table 7**). These data demonstrate that increased NREM (N2 + N3) sleep duration contributes
441 to the overnight clearance of Aβ and tau to the plasma.

442

443 *Combined effects of release and clearance to plasma Aβ and tau levels during sleep deprivation*

444 We next evaluated whether the neurophysiological features used to characterize sleep also
445 influenced Aβ and tau release and clearance under conditions of overnight sleep deprivation
446 (waking). To address this, we constructed the single-index predictor ***Physio$_W$*** from the same
447 regressors, optimizing it to best fit the sleep deprivation data (**Table 4**). The **null model** and the
448 **neuro-glymphatic model** fitted to morning plasma AD biomarker levels following sleep
449 deprivation, using the single predictor ***Physio$_W$*** are shown **Supplemental Table 11**. By
450 incorporating overnight neurophysiological features related to glymphatic exchange and
451 synaptic-metabolic activity into ***Physio$_W$***, the **neuro-glymphatic model** demonstrated superior
452 predictive performance for morning plasma AD biomarker levels compared with the null model
453 (**Table 6**, LRT, $p < 0.001$). When assessing the additional variance in morning plasma Aβ and
454 tau levels explained by the **neuro-glymphatic model** beyond that explained by the **null model**,
455 we found that in amyloid-positive individuals the model accounted for 72.8% of all tau variance.
456 In amyloid-negative individuals, the model explained 92.5% of Aβ40, 93.3% of Aβ42, and 73.8%
457 of p-tau181 variance (**Table 7**).

458

459 In individuals undergoing overnight sleep deprivation, HRV, PTT, and R_P measures contributed
460 to Aβ and tau release and clearance in a manner largely consistent with their effects during
461 sleep, although the contribution of R_P was substantially smaller (**Supplementary Table 3**). In
462 this context, increases in EEG delta and theta power were associated with elevated Aβ and tau
463 release, whereas a reduction in EEG beta power enhanced clearance, an association previously
464 observed in both rodent and human studies[17,22]. Note that in amyloid-positive individuals,
465 predictor assignment for a decrease in ***Physio$_W$*** was based on all tau effects (**Supplemental**
466 **Table 8**), as Aβ40 and Aβ42 effects were not statistically significant (**Supplemental Table 11**).

467 These data suggest that under conditions of sleep deprivation, both synaptic-metabolic release
468 and glymphatic clearance of Aβ and tau contribute to morning plasma AD biomarker levels.
469
470 *The predictors **Physio$_S$**, **Hypno$_S$** and **Physio$_W$** in the neuro-glymphatic model replicate the rate*
471 *constants in the compartmental pharmacokinetic model*
472 The linear interaction terms between the predictors ***Physio$_S$***, ***Hypno$_S$*** and ***Physio$_W$*** and evening
473 plasma AD biomarker levels in the three **neuro-glymphatic models** for amyloid-positive and
474 amyloid-negative individuals were significant at both the group level (**Table 8**) and individual
475 levels (**Table 5, Supplemental Tables 5-6**). These interaction terms are the same as described
476 by **Equation 3** in the solution of the multi-compartment model (**Supplementary Methods and**
477 **Results**). That is, the linear interaction terms between the predictors ***Physio$_S$***, ***Hypno$_S$*** and
478 ***Physio$_W$*** and evening plasma AD biomarker levels from experimental observations are
479 consistent with those derived from multicompartment first-order kinetic modeling under the
480 **neuro-glymphatic model** assumption with ISF to CSF clearance rate constants and synaptic-
481 metabolic release that are time-varying through ***Physio$_S$***, ***Hypno$_S$*** and ***Physio$_W$***.
482
483 To further demonstrate this correspondence, we compared experimental predictions of morning
484 plasma AD biomarker levels when ***Physio$_S$*** and ***Hypno$_S$*** were varied by ±1 standard deviation
485 with predictions generated by the compartmental model under proportional variation of the rate
486 constants k_{glymph_out}, k_{glymph_in} and k_{cell_rel}. As shown in **Figure 3A–B**, varying the magnitude
487 of fitted predictors in the **neuro-glymphatic models** for sleep, while proportionally varying
488 k_{glymph_out} and k_{glymph_in} in the compartment model, produced similar changes in predicted
489 morning plasma AD biomarker levels across all conditions. Furthermore, the compartmental
490 model reproduced the experimentally-observed pattern of greater clearance of aggregation-
491 prone species (Aβ42, p-tau181) relative to non-aggregation-prone species (Aβ40, np-tau181),

492 consistent with an increased Aβ42/Aβ40 and p-tau181/np-tau181 ratio over baseline clearance.
493 By contrast, increasing k_{cell_rel} in the compartmental model generated similar directional effects
494 on morning plasma biomarker levels but reduced clearance of aggregation-prone species
495 relative to non-aggregation-prone species, a pattern inconsistent with the experimental
496 predictions (**Figure 1, Supplemental Table 1**). Taken together, these findings support
497 glymphatic clearance as the predominant physiological mechanism underlying the observed
498 variation in morning plasma AD biomarker levels following overnight sleep.
499
500 We next compared experimental predictions of morning plasma AD biomarker levels during
501 sleep deprivation, obtained by varying ***Physio$_W$*** by ±1 standard deviation, with predictions from
502 the compartment model under proportional variation of the rate constants k_{glymph_out}, k_{glymph_in}
503 and k_{cell_rel}. As shown in **Figure 3C**, reproducing the experimental results from the **neuro-**
504 **glymphatic models** required varying k_{cell_rel} in the compartmental model. This adjustment
505 produced similar changes in predicted morning plasma AD biomarker levels and replicated the
506 experimentally-observed pattern of reduced clearance of aggregation-prone species (Aβ42, p-
507 tau181) relative to non-aggregation-prone species (Aβ40, np-tau181). Thus, under sleep
508 deprivation, increased synaptic-metabolic release emerges as the predominant physiological
509 mechanism underlying the observed morning plasma AD biomarker levels.
510
511 It is noteworthy that while the results of the statistical and compartmental models converge, they
512 were derived from independent sources. The glymphatic models were statistically estimated
513 from the experimental data from the Villages and UW clinical studies whereas the
514 compartmental model was based on the elimination kinetics of amyloid β and tau obtained from
515 independent published research[27,28].
516

517 **DISCUSSION**

518 We developed a compartmental transport model based on published kinetic values to predict
519 the effect that sleep-active glymphatic CSF-ISF exchange and synaptic-metabolic activity has
520 on overnight changes in plasma Aβ and tau levels. To rigorously test the glymphatic model of
521 interstitial Aβ and tau clearance from the human brain during sleep, and to define the relative
522 contributions that changes in synaptic-metabolic release and clearance make to plasma Aβ and
523 tau levels, we conducted a multi-site, randomized, crossover clinical study. This study utilized a
524 novel investigational device from Applied Cognition[17] to measure parenchymal resistance R_P,
525 sleep EEG features, cerebrovascular pulse transit time PTT, heart rate variability HRV, in
526 addition to clinically validated blood-based biomarkers of Aβ and tau provided by C2N[32-34].
527 Healthy older participants underwent both overnight sleep and sleep deprivation visits. Our
528 findings showed that reduced parenchymal resistance, increased cerebrovascular compliance,
529 and elevated EEG delta power during NREM sleep – each of which are associated with
530 increased glymphatic function in rodents and humans[12,13,17,22,23,25,40] – predicted higher morning
531 plasma levels of Aβ and tau. EEG theta power during NREM sleep, and both theta and beta
532 power during REM sleep, also contributed to morning plasma Aβ and tau levels, though to a
533 lesser extent, suggesting a role for synaptic–metabolic activity in Aβ and tau release to the
534 plasma[29-31]. These predictors of sleep-active glymphatic clearance and synaptic–metabolic
535 release explained over 50% of the residual variance in morning plasma AD biomarker levels
536 among amyloid-positive individuals, and over 90% among amyloid-negative individuals, that
537 was not explained by the model that assumed constant overnight CSF–ISF exchange and
538 reduced but uniform synaptic–metabolic activity across individuals.

539

540 The burden of Aβ and phosphorylated tau in the brain is diagnostic for AD and prognostic of its
541 progression[42-44]. Recently approved monoclonal antibody therapies targeting Aβ demonstrate

542 marked reduction in brain Aβ burden, but at present provide only modest improvement in
543 cognitive outcomes and quality of life[45,46]. This apparent shortcoming has led to an increasing
544 interest in extending anti-Aβ immunotherapy into earlier, preclinical stages of AD and into at-risk
545 populations such as *APOE-ε4* carriers. It is also possible that if the mechanisms contributing to
546 the development and progression of Aβ and tau pathology can be defined, then it may be
547 possible both to better identify individuals at risk of the development of this pathology and to
548 intervene in at-risk individuals to prevent its development and eventual progression.
549
550 In rodent models, sleep-active glymphatic function has been implicated in the clearance of both
551 Aβ and tau. Interstitial Aβ and tau both move through brain tissue along perivascular
552 pathways[10,14], while inhibition of glymphatic function by either *Aqp4* or *Snta1* gene deletion
553 slows the clearance of Aβ and tau and promotes the development of Aβ and tau pathology[10,13-
554 15,47-51]. Glymphatic function is impaired in animal models of aging[52], cerebrovascular
555 dysfunction[53,54], traumatic brain injury[14,55-57], and sleep disruption[13,58]; each of which are non-
556 genetic risk factors for Alzheimer's disease. This body of results from rodent studies suggests
557 that impairment of glymphatic clearance of Aβ and tau is a key factor in the development of AD,
558 serving as a mechanistic linkage between a wide spectrum non-genetic AD risk factors and the
559 development of AD-related Aβ and tau pathology[59,60]. If true, then the detection of glymphatic
560 impairment would permit the identification of individuals at risk for the development of Aβ and
561 tau pathology, while targeting glymphatic function would provide a novel approach to the
562 prevention of the development and progression of AD pathology in at-risk individuals.
563
564 Despite promising results from rodent studies, key biological features of sleep-active glymphatic
565 function have only recently been confirmed in the human brain. Intrathecal contrast-enhanced
566 MRI studies have demonstrated extensive CSF-ISF exchange in the human brain[61], that this

567 exchange is organized along the axis of the cerebral arterial vasculature[62], and that ISF solute
568 clearance is more rapid in the sleeping compared to the waking brian[16]. In a recent study, we
569 demonstrated that glymphatic function is sleep-active, and enhanced during sleep by increasing
570 EEG delta power, reduced EEG beta power, reduced HR, and reduced parenchymal resistance
571 R_P[17]. Yet a role for sleep active glymphatic exchange in the clearance of Aβ and tau from the
572 human brain remains largely undefined.
573
574 One recent study by Lucey and colleagues reported that the CSF-to-blood clearance of Aβ and
575 tau are impaired by acute sleep deprivation[4], although this study did not specifically implicate
576 glymphatic clearance in this association. In another important study by Eide et al.[21], the authors
577 report that in participants undergoing assessment of glymphatic function and CSF-to-plasma
578 clearance by intrathecal contrast-enhanced MRI, slowed glymphatic clearance was associated
579 with lower plasma total-tau levels, while slowed CSF-to-plasma clearance was correlated with
580 lower Aβ42 levels. While this study supports a role for glymphatic exchange in the clearance of
581 AD-related biomarkers, the interpretation of the findings has key limitations. Because intrathecal
582 administration is an off-label use of gadolinium-based contrast agents such as gadobutrol, the
583 study was carried out in participants being evaluated for disordered CSF circulation and not
584 otherwise 'healthy' participants. This introduced a several decade age range and multiple
585 clinical indications in the study group that would be expected to confound the relationship
586 between plasma levels of AD biomarkers and glymphatic function. While the study did evaluate
587 the effect of time of day on plasma biomarker levels, the relationship between measures of
588 glymphatic clearance and overnight dynamic changes in AD biomarker levels, rather than
589 'steady state' levels, was not evaluated. Lastly, while overall self-reported sleep quality was
590 evaluated with the Pittsburgh Sleep Quality Index, objective measures of sleep parameters,
591 sleep stages, or sleep EEG spectral band powers were not evaluated. In the present study, we

592 extend these initial studies by evaluating the effect of overnight parenchymal resistance, sleep
593 stages, sleep EEG powerbands during REM and NREM, cerebrovascular arterial compliance
594 and heart-rate variability, each of which is a key determinate of glymphatic
595 transport[12,13,17,22,23,25,40,41] or a key contributor to synaptic-metabolic release[29-31], on the dynamic
596 clearance of Aβ and tau to the plasma in healthy older individuals.
597
598 To test whether sleep-active glymphatic function contributes to the clearance of Aβ and tau from
599 the human brain independent of variations in synaptic-metabolic activity during sleep, we first
600 developed a multicompartment model of Aβ and tau clearance from the brain interstitium. The
601 model was designed to predict the effects of sleep-related changes in glymphatic CSF–ISF
602 exchange and synaptic–metabolic release on evening-to-morning changes plasma Aβ and tau
603 levels. Glymphatic clearance was modeled as changes in the rate constants between ISF and
604 CSF compartments, demonstrating that an overnight increase in exchange would result in
605 higher plasma AD biomarker levels the following morning. Similarly, synaptic–metabolic release
606 was modeled as a change in the rate constant for Aβ and tau release from cells into the ISF,
607 which also predicted elevated morning plasma biomarker levels when release increased.
608
609 Monomeric Aβ42 and p-tau181 in the ISF were modeled as being in equilibrium with their non-
610 monomeric forms using a separate compartment and published rate constants between ISF and
611 aggregate pools[27,28]. This revealed that an increase (or decrease) in the exchange rate between
612 ISF and CSF (glymphatic exchange) preferentially increased (or decreased) the clearance of
613 aggregation-prone species (Aβ42 and p-tau181) relative to non-aggregation-prone species
614 (Aβ40 and np-tau181). In contrast, increasing the release rate from cells into the ISF led to the
615 opposite effect, preferentially elevating non-aggregation-prone over aggregation-prone species.
616 These key differences in model behavior allowed us to directly test the hypothesis that

617 glymphatic clearance of Aβ and tau is the dominant contributor to sleep-related variation in
618 plasma Aβ and tau levels, while synaptic–metabolic release dominates during sleep deprivation
619 (and likely waking).
620
621 Analyzing data from two cross-over design clinical studies, we evaluated the validity of two
622 parallel models to explain overnight changes in plasma Aβ and tau levels. Our **null hypothesis**
623 was that neither glymphatic exchange nor synaptic-metabolic release contributed to the
624 overnight changes in AD plasma biomarkers, and the **null model** used only the evening AD
625 plasma biomarker levels adjusted by biological confounders to predict the morning AD
626 biomarker levels. The **neuro-glymphatic hypothesis** was that increased CSF-ISF exchange
627 during sleep increased the overnight clearance of Aβ and tau from brain to the plasma and that
628 individual differences in overnight synaptic-metabolic release further altered morning plasma
629 levels. Because glymphatic function and synaptic-metabolic activity during sleep are regulated
630 by changes in EEG delta, theta and beta power during NREM and REM, and PTT, HRV, and
631 R_P[12,13,17,22,23,25,29-31,40,41], we tested if the inclusion of these features would improve the prediction
632 of plasma Aβ and tau levels consistent with our multicompartment model prediction.
633
634 Using a single-index regression that linearly combined these variables into single predictor
635 ***Physio$_S$*** for sleep, the **neuro-glymphatic model** explained over 50% of the residual variance in
636 morning plasma AD biomarker levels in amyloid-positive individuals and over 90% in amyloid-
637 negative individuals during the sleep condition. The optimal sleep predictor ***Physio$_S$*** which
638 maximized the log-likelihood during sleep, was primarily driven by parenchymal resistance R_P,
639 with smaller contributions from cerebrovascular compliance measure by PTT and EEG delta
640 power during NREM sleep, features associated with increased glymphatic clearance. Minor

641 contributions also came from EEG theta power during both NREM and REM sleep, and EEG
642 beta power during REM, features suggestive of increased synaptic-metabolic release.
643
644 During the sleep deprivation (awake) condition, the **neuro-glymphatic model** with the optimal
645 predictor ***Physio$_W$*** accounted for over 70% of np-tau and p-tau variance in amyloid-positive
646 individuals, and between 70% and 90% of Aβ and p-tau variance in amyloid-negative
647 individuals. HRV, PTT, and R_P contributed to the predictor ***Physio$_W$*** in a manner largely
648 consistent with their effects during sleep on glymphatic clearance, although R_P showed a
649 substantially smaller contribution. In contrast to the optimal sleep predictor, however, EEG delta,
650 theta and beta power that are associated with increased synaptic-metabolic production during
651 wake, contributed strongly to ***Physio$_W$*.**
652
653 When we tested the **neuro-glymphatic model** using the single-index predictor ***Hypno$_S$*** for the
654 sleep condition, constructed from sleep stage durations, it did not outperform the null model in
655 explaining Aβ40 and Aβ42 levels in amyloid-negative individuals, although it did explain over
656 64% of the variance in tau level. In amyloid-positive individuals, ***Hypno$_S$*** explained over 30% of
657 the variance. Increased NREM (N2+N3) sleep duration, associated with enhanced glymphatic
658 clearance, and decreased REM sleep, N1 sleep, and WASO, associated with increased
659 synaptic-metabolic release, contributed to ***Hypno$_S$***. That sleep stage duration alone showed
660 poorer performance in explaining overnight changes in plasma Aβ and tau levels is not
661 surprising. Measuring variations in the underlying neurophysiology occurring in each sleep
662 stage is likely to be more predictive than simply quantifying time spent in each stage.
663
664 While it is widely appreciated that glymphatic clearance is more rapid during sleep than during
665 waking, glymphatic clearance does occur during wake[13,17]. Yet to what extent this clearance is
666 modifiable by sleep-like physiology during waking has remained unknown. Sleep deprivation

667 also increases Aβ and tau release into the ISF[29-31]. The wake prediction model using ***Physio$_W$***
668 was notable in that it explained a substantial amount of the overnight variance in plasma Aβ and
669 tau levels, with contributions from both increased glymphatic clearance and increased release.
670 The optimal single predictor, ***Physio$_W$***, showed that changes in cerebrovascular compliance,
671 sympathetic/noradrenergic tone, and parenchymal resistance contributed to increased
672 glymphatic clearance, similar to their effects during sleep in ***Physio$_S$***. In contrast, wake EEG
673 theta and delta power were associated with increased synaptic-metabolic release. While
674 increased glymphatic clearance during wakefulness contributed to morning Aβ and tau levels,
675 simulated changes in the **neuro-glymphatic model's** single-index predictor ***Physio$_W$*** produced
676 predicted shifts in plasma AD biomarker levels that were consistent with release being the
677 primary driver. This interpretation aligns with the multicompartment model, which showed similar
678 results when comparable magnitude changes were made to the cell-to-ISF release rate
679 constant.
680
681 We were further able to show from these data that a simulated change in the **neuro-glymphatic**
682 **model *Physio$_S$*** or ***Hypno$_S$*** single-index predictors led to predicted changes in Aβ and tau
683 clearance to plasma that replicated the predictions made by the multicompartment model when
684 similar magnitude changes were made to the CSF-ISF rate constants. Considering that the
685 multicompartment model was derived from external published data[27,28], this finding
686 independently corroborates the findings from our experimental data and statistical model. It is
687 also noteworthy that the interaction between the single-index predictor and evening plasma
688 concentration in the *experimental* **neuro-glymphatic model** mirrored the interaction between
689 the CSF-ISF and cellular release rate constants and evening plasma concentration in the
690 *multicompartment* **neuro-glymphatic model**. This suggests an association between these rate
691 constants and the neurophysiological or hypnogram measures identified by the single-index

692 predictors. Together these results affirm the **neuro-glymphatic model**, that increased synaptic-
693 metabolic release and glymphatic clearance during sleep supports overnight changes in plasma
694 Aβ and tau levels. These findings further support the predominance of sleep-active glymphatic
695 clearance of Aβ and tau from the brain during sleep, and highlight a key role for synaptic-
696 metabolic production of Aβ and tau during sleep-deprivation.
697
698 In addition to supporting the role for glymphatic transport in the clearance of Aβ and tau during
699 sleep, the present results provide additional mechanistic insights into how these processes
700 unfold in the human brain. Consistent with prior studies in rodents and humans, EEG delta
701 power[13,17,22,23] during NREM sleep and increased cerebrovascular compliance[12,25,40] contributed
702 to increasing clearance of Aβ and tau to the plasma in the overnight period, while higher EEG
703 theta and delta power during REM sleep contributed to increasing synaptic-metabolic release[29-
704 31]. These contributions are in marked contrast to the dominant effect that R_P had within these
705 models, with lower overnight R_P contributing to greater morning plasma Aβ and tau levels, which
706 may be because R_P mediates the downstream effect of these variables. Conceptually, the
707 synchronized low-frequency neural activity reflected in delta band power and increases in
708 cerebrovascular compliance may serve as a key driving force for the process of glymphatic
709 clearance, while astroglial-mediated changes in extracellular volume fraction reflected in the R_P
710 parameter[13,17] may regulate the effects of this driving force on fluid and solute transport within
711 the brain parenchyma. If true, then R_P may represent a promising therapeutic target to increase
712 glymphatic clearance of Aβ and tau.
713
714 It is important to point out the distinction between the changes in plasma AD biomarker levels
715 observed through a single overnight period in the present study and changes in plasma AD
716 biomarker levels that reflect steady-state alterations in AD-related pathology. For example, over

717 the timescale of years, declining plasma Aβ42 levels and increasing p-tau levels occur with
718 increasing Aβ plaque and tau pathological burden in AD. Within the setting of the present study,
719 overnight changes in plasma AD biomarker levels reflect the dynamics of both the release of Aβ
720 and tau species into the brain interstitium, and their subsequent clearance to the CSF and the
721 plasma in the overnight period. These dynamics are superimposed upon the existing steady-
722 state Aβ42 and p-tau levels of each participant that were analyzed separately for amyloid-
723 positive and amyloid-negative individuals. Within these two groups, we do not expect individual
724 overnight differences in Cell-ISF release and CSF-ISF exchange to be affected by baseline
725 Aβ42 and p-tau levels. The converse question – whether impaired overnight Aβ and tau
726 clearance leads to increased AD pathological burden and long-term shifts in steady-state
727 plasma AD biomarker levels – is a compelling hypothesis that requires a further investigation.
728
729 Our findings showed that elements of sleep-active physiology, in particular, brain parenchymal
730 resistance, enhanced the clearance of Aβ and tau into plasma during overnight sleep in
731 humans. In contrast, during sleep deprivation, increased synaptic–metabolic release elevated
732 plasma AD biomarker levels overnight. Our **null model** and **neuro-glymphatic model** were
733 estimated to predict morning AD biomarker levels from evening AD biomarker levels which is
734 statistically superior to estimating those models on morning-to-evening differences or ratios of
735 AD biomarker levels[63]. We further showed that while synaptic-metabolic release was dominant
736 in the awake state, sleep-related physiology also contributed to increasing Aβ and tau clearance
737 to the plasma.
738

SUPPLEMENTAL METHODS AND RESULTS

Derivation of compartmental pharmacokinetic model

The movement of solute across the compartments in **Figure 1A** can be modeled using first-order kinetics with the published rate constants shown in **Table 1**. This leads to the following linear system of first-order differential equations where f is the cellular production of APP or tau that was assumed to be constitutive, time-independent, across sleep/wake cycles[29,30]:

$$\frac{dy_1}{dt} = -k_{cell_rel}(y_1 - C) + f$$

$$\frac{dy_2}{dt} = -(k_{glymph_out} + k_{24} + k_{25} + k_{on-rate})y_2 + k_{cell_rel}y_1 + k_{glymph_in}y_3 + k_{off-rate}y_6$$

$$\frac{dy_3}{dt} = -(k_{glymph_in} + k_{34})y_3 + k_{glymph_out}y_2$$

$$\frac{dy_4}{dt} = -k_{4e}y_4 + k_{24}y_2 + k_{34}y_3$$

$$\frac{dy_5}{dt} = -k_{52}y_5 + k_{25}y_2$$

$$\frac{dy_6}{dt} = -k_{off-rate}y_6 + k_{on-rate}y_2$$

and in matrix notation,

$$\frac{d\vec{y}}{dt} = A\vec{y} + (f + k_{cell_rel}C)\vec{u}_1 \quad \textbf{Eq (1)}$$

$$A = \begin{bmatrix} -k_{cell_rel} & 0 & 0 & 0 & 0 & 0 \\ k_{cell_rel} & -(k_{glymph_out} + k_{24} + k_{25} + k_{on-rate}) & k_{glymph_in} & 0 & 0 & k_{off-rate} \\ 0 & k_{glymph_out} & -(k_{glymph_in} + k_{34}) & 0 & 0 & 0 \\ 0 & k_{24} & k_{34} & -k_{4e} & 0 & 0 \\ 0 & k_{25} & 0 & 0 & -k_{52} & 0 \\ 0 & k_{on-rate} & 0 & 0 & 0 & -k_{off-rate} \end{bmatrix}$$

where $\vec{u}_1$ is the unit vector $(1,0,0,0,0,0)$.

Equation 1 was solved numerically using the *mrgSolve* in *R*. Peptides and proteins released from the Cell compartment to enter the ISF will be cleared from the ISF to the various

compartments in a time-dependent manner modeled by $\vec{y}(t)$. The **null model** assumes, in the absence of sleep-active glymphatic exchange between the ISF and CSF, that the rate constants k_{glymph_out} and k_{glymph_in} are not time dependent. This model further assumes that the rate of release k_{cell_rel} of Aβ and tau from the cell to the ISF compartment during sleep was constant at 30% lower than during wake, and during sleep deprivation was 10% lower than during wake due to circadian regulation.

In contrast, the **neuro-glymphatic model** relaxes the constraint of time-independent rate constants k_{glymph_out} and k_{glymph_in}, which are now allowed to increase during sleep, reflecting the increased CSF solute influx and interstitial solute efflux observed in the rodent and human brain[13,16,17]. Furthermore, the Cell release rate k_{cell_rel} of Aβ and tau into the ISF is allowed to vary during sleep and sleep-deprivation reflecting individual changes in synaptic-metabolic production[29-31].

We then solved the simulation model for $\vec{y}(t)$ under the **null model** condition and then under the **neuro-glymphatic model** under two scenarios. The first scenario increased the rate constants k_{glymph_out} and k_{glymph_in}, and separately increased the Cell release rate constant k_{cell_rel} to define whether morning plasma Aβ and tau levels increase with more rapid overnight glymphatic CSF-ISF exchange or with greater overnight synaptic-metabolic activity.

Of final interest is the solution of a linear approximation of **Equation 1** for the morning compartment concentrations $\vec{y}(t_{AM})$ as a function of the evening compartment concentrations $\vec{y}(t_{PM})$. With overnight rate constants k_{glymph_out}, k_{glymph_in} and k_{cell_rel} in the **neuro-glymphatic model** held at either increased or decreased level relative to the **null model,** and letting $\Delta t =$

$t_{AM} - t_{PM}$ represent the fixed time between the two blood samples, we apply the fundamental matrix and variation of parameters to solve **Equation 1,** yielding

$$\vec{y}(t_{AM}) = e^{A\Delta t}\vec{y}(t_{PM}) + A^{-1}(e^{A\Delta t} - I)\vec{b}$$

where $\vec{b} = \left(f + k_{cell_rel}C\right)\vec{u}_1$. The **neuro-glymphatic model** allows for k_{glymph_out}, k_{glymph_in} and k_{cell_rel} in A to vary around their fixed values in the **null model**. We are interested in the effect that varying these rate constants has on $\vec{y}(t_{AM})$. Letting ∂A denote a matrix of small variations of k_{glymph_out}, k_{glymph_in} and k_{cell_rel}

$$\partial A = \begin{bmatrix} -\partial k_{cell_rel} & 0 & 0 & 0 & 0 & 0 \\ \partial k_{cell_rel} & -\partial k_{glymph_{out}} & \partial k_{glymph_in} & 0 & 0 & 0 \\ 0 & \partial k_{glymph_out} & -\partial k_{glymph_in} & 0 & 0 & 0 \\ 0 & 0 & 0 & 0 & 0 & 0 \\ 0 & 0 & 0 & 0 & 0 & 0 \\ 0 & 0 & 0 & 0 & 0 & 0 \end{bmatrix}$$

we solve for the first-order approximation of

$$\vec{y}(t_{AM}) = e^{A\Delta t + \partial A\Delta t}\,\vec{y}(t_{PM}) + (A + \partial A)^{-1}(e^{A\Delta t + \partial A\Delta t} - I)\vec{b}$$

Using the Fréchet derivative, a first order approximation gives

$$y(t_{AM}) - e^{A\Delta t}\vec{y}(t_{PM}) \propto (\partial A\Delta t + \tfrac{1}{2}(A \cdot \partial A - \partial A \cdot A)\Delta t^2)\vec{y}(t_{PM})e^{A\Delta t} \qquad \textbf{Eq (3)}$$

We observe that $e^{A\Delta t}\vec{y}(t_{PM})$ is the multicompartment **null model** prediction of $\vec{y}(t_{AM})$ and the right-hand side of **Eq (3)** gives the first-order contribution to $\vec{y}(t_{AM})$ of the **neuro-glymphatic model** solution of the multi-compartment model that arises from varying the rate constants k_{glymph_out}, k_{glymph_in} and k_{cell_rel}. We note that this effect is linear in k_{glymph_out}, k_{glymph_in} and k_{cell_rel}, capturing the interaction between evening plasma biomarkers levels $\vec{y}(t_{PM})$ and both glymphatic CSF-ISF exchange and synaptic-metabolic cellular release in the **neuro-glymphatic model** versus the **null model**. In summary, in the **null model,** morning plasma levels are linearly dependent on evening plasma levels only, whereas the **neuro-glymphatic model** has a

806 contribution from the interaction term between the evening plasma levels and the variable rate
807 constants k_{glymph_out}, k_{glymph_in} and k_{cell_rel}.
808
809 *Plasma AD biomarker assessment*
810 The *APOE* genotyping, Aβ and tau plasma biomarkers were analyzed using mass spectrometry
811 by C_2N Diagnostics[64]. The sample collection procedure was provided by C_2N Diagnostics.
812 Venipuncture and blood draw from the antecubital fossa were performed using a 22-gauge
813 butterfly needle to minimize red blood cell hemolysis. A total of 10 ml of blood was drawn into a
814 K_2 EDTA Vacutainer. The blood was centrifuged for 15 min using a swinging bucket rotor at
815 500-700 x g with the brake on. Immediately after centrifugation, four 1.0 mL plasma samples
816 were aliquoted into four Sarstedt 2.0 ml Micro Tubes without disrupting the plasma/cell interface
817 when transferring plasma. A calibrated air-displacement hand-held pipette with a polypropylene
818 pipette tip was used. After aliquoting plasma into the Sarstedt Micro Tubes, the tubes were
819 immediately capped and frozen at -40°C. When the tubes were ready to be shipped to C_2N
820 Diagnostics, they were packed into a plastic zip-lock bag with plenty of dry ice, placed in an
821 absorbent towel **and** cryobox, and express couriered to C_2N Diagnostics priority overnight.
822
823 *Validation of PTT measures of cerebrovascular function*
824 The cerebrovascular pulse transit time (PTT) was computed using data acquired from the
825 impedance plethysmogram (IPG) and the left-ear photoplethysmogram (PPG) sensors of the
826 investigational device[17]. A digital filter was applied to the signal in both forward and backward
827 directions using Python SciPy's filtfilt function, resulting in zero phase distortion. The signal was
828 then bandpass-filtered between 0.5 Hz and 10 Hz using a finite impulse response (FIR) filter
829 with a Hann window (firwin in Python SciPy).
830

The signal troughs of the IPG measured intracranial cerebrovascular pulsations, while the PPG troughs captured peripheral vascular pulsations. The time difference between the IPG and PPG troughs was calculated as the beat-to-beat cerebrovascular PTT. These intervals were averaged over 30-second EEG epochs.

For the sleep condition, cerebrovascular PTT was expressed as the overnight mean of epoch PTTs normalized to the average PTT of the first three sleep epochs. For the sleep deprivation/wake condition, cerebrovascular PTT was similarly averaged and normalized using the first three wake epochs. Peripheral vascular PTT was computed analogously, using the time difference between the left-ear and right-ear PPG signals[65]. Cerebrovascular PTT during NREM sleep was calculated exclusively over N2 and N3 sleep epochs.

Cerebral blood volume (CBV) was measured the following morning after completion of either the overnight sleep or sleep-deprivation period. A contrast-enhanced, steady-state MRI technique was employed, with normalization to the superior sagittal sinus to obtain absolute CBV values[66]. CBV was measured in eight regions of interest (ROIs): the gray and white matter of the frontal, parietal, temporal, and occipital lobes.

Hemodynamic Relationships and Physiological Interpretation

The relationship between mean arterial pressure (MAP) and peripheral PTT is well-established and inversely proportional:

$$\downarrow \textbf{MAP} \rightarrow \uparrow \textbf{Peripheral PTT}$$

The relationship between MAP and cerebrovascular PTT is similar but more complex due to cerebral vascular autoregulation, which maintains constant cerebral blood flow (CBF) over a wide range of cerebral perfusion pressures (CPP). CPP is defined as:

$$\textbf{CPP} = \textbf{MAP} - \textbf{ICP}$$

where ICP is intracranial pressure.

Due to autoregulation:

↓MAP → ↑CBV → ↑ICP → ↓Transmural ΔP → ↑Cerebrovascular PTT

An increase in CBV raises ICP. When this is combined with a decreased MAP, the resulting drop in transmural pressure leads to increased cerebrovascular PTT.

In contrast, when MAP increases:

↑MAP → ↓Peripheral PTT

In the peripheral vasculature, higher MAP increases transmural pressure, reducing PTT. In the cerebrovascular system, increased MAP leads to:

↑MAP → ↓CBV → ↓ICP → ↑Transmural ΔP → ↓ Cerebrovascular PTT

Here, cerebral autoregulation reduces CBV (and ICP) in response to higher MAP, increasing transmural pressure and reducing cerebrovascular PTT.

These mechanisms assume constant brain metabolic demand, under which CBV and cerebrovascular PTT are positively correlated. However, when brain metabolic demand decreases, such as during NREM sleep (assuming MAP remains unchanged):

↓Metabolic Demand → ↑Cerebrovascular Tone → ↓CBV → ↓ICP → ↑Transmural ΔP → ↓Cerebrovascular PTT

In this case, decreased metabolic demand reduces CBF via increased vascular tone, leading to reduced CBV and ICP, which in turn increases transmural pressure and reduces cerebrovascular PTT.

Thus, we conclude that cerebral autoregulation maintains a positive association between cerebral blood volume (CBV) and cerebrovascular pulse transit time (PTT) under both

883 fluctuations in mean arterial pressure (MAP) and changes in brain metabolic demand. However,
884 it is important to note that MAP and metabolic demand can vary independently or in opposing
885 directions.
886
887 **Supplemental Table 2** presents the overnight sleep and wake peripheral PTT and
888 cerebrovascular PTT in amyloid-positive and amyloid-negative participants. While the sleep-to-
889 wake differences are not statistically significant, likely due to the small sample size, the
890 observed trends offer valuable insights.
891
892 Among amyloid-negative participants, peripheral PTT increased during sleep compared to
893 wakefulness. This pattern aligns with a decrease in MAP during sleep, which, assuming
894 metabolic demand remains constant, would increase CBV and, consequently, increase
895 cerebrovascular PTT. However, sleep is also characterized by reduced brain metabolic
896 demand, which tends to decrease CBV and lower cerebrovascular PTT. These opposing
897 physiological effects appear to offset each other, resulting in minimal net change in
898 cerebrovascular PTT between sleep and wake in this group.
899
900 In contrast, amyloid-positive participants showed a decrease in peripheral PTT during sleep
901 relative to wakefulness. This trend suggests an increase in MAP during sleep, which would
902 reduce CBV. Combined with the reduction in metabolic demand during sleep, which also lowers
903 CBV, the additive effect would be a decrease in cerebrovascular PTT, a finding that is
904 consistent with the values shown in **Supplemental Table 2**.
905
906 To test the hypothesis that overnight cerebrovascular PTT predicts morning CBV, we employed
907 a multivariate linear mixed-effects model. This model included eight dependent CBV variables,
908 one for each region of interest (ROI), and a single independent predictor: cerebrovascular PTT.

909 Potential confounding variables were included in the model: age, sex, APOE ε4 carrier status,
910 and circadian alignment, as previously described. All participants were drawn from the
911 Benchmarking Study; participants in the Replication Study were excluded from this analysis, as
912 they did not undergo contrast-enhanced MRI and therefore had no CBV measurements
913 available.
914
915 The regression coefficients for cerebrovascular PTT in the multivariate linear mixed model were
916 positive and statistically significant across all eight ROIs for amyloid-negative participants, both
917 following overnight sleep and overnight sleep deprivation (**Supplemental Tables 3 and 4**).
918 These findings are consistent with the proposed positive physiological relationship between
919 CBV and cerebrovascular PTT.
920
921 In amyloid-positive participants, the cerebrovascular PTT coefficients were also positive and
922 significant across all eight ROIs following overnight sleep deprivation, and positive and
923 significant for the four gray matter ROIs following overnight sleep (**Supplemental Tables 3 and**
924 **4**).
925
926 Model performance was evaluated by comparing the prediction model, which included
927 cerebrovascular PTT, against a null model that excluded cerebrovascular PTT. The likelihood
928 ratio test (LRT) indicated that the prediction model provided a significantly better fit across all
929 four comparisons: amyloid-positive vs. amyloid-negative and sleep vs. sleep deprivation
930 (**Supplemental Table 5**).
931
932 Using the marginal variances for each model that reflect the total population-level variance of
933 between-subject variation and within-subject variation, the prediction model explained between
934 63.8% and 85.4% of the variance attributed to the **null model** across the eight regions of

935 interest (ROIs) in each of the four comparisons[67]. Similarly high percentages of variance were
936 explained when analyzed by individual ROI (**Supplemental Table 6**).
937
938 *Construction of Single Predictors*
939 The objective of the single-predictor approach, using single-index regression[34], was to identify a
940 single linear combination of predictors that would allow inferences about the relative
941 contributions of glymphatic clearance and synaptic–metabolic release variables in explaining
942 plasma biomarker levels within the **neuro-glymphatic model**. Given the inferential nature of the
943 hypotheses, all variables were retained, and models were selected based on maximum log-
944 likelihood. The construction proceeded through two steps: **1)** identifying a maximal non-collinear
945 subset of the predictor regressors from the appropriate group of regressors; **2)** running an
946 optimization algorithm to find the weights for the linear combination that minimized the log-
947 likelihood of the **neuro-glymphatic model** on the data[68]. Optimization was performed using the
948 R optim function with Nelder-Mead optimization. Each optimization was run with multiple initial
949 parameter values and the best result selected. Once the best single predictor subset of
950 regressors and weights were determined for $\boldsymbol{Physio_S}$, $\boldsymbol{Physio_W}$ and $\boldsymbol{Hypno_S}$, Wald's p values
951 and 95% CI were estimated on each of the weights using 1,000 bootstrap re-samples. The R
952 package *lmeresampler* for bootstrap routines for nested linear mixed effects models was used
953 to resample the data.
954
955 *Multivariate model representing the null model and neuro-glymphatic models*
956 The R lme4 package was used for the linear mixed models. The multivariate linear mixed model
957 was modeled in lme4[69].
958

959 The **null model** represented the null hypothesis that efflux of Aβ and tau from the ISF to the
960 CSF is not dependent on glymphatic exchange, that is, k_{glymph_out} and k_{glymph_in} are time-
961 invariant. Furthermore, in this model efflux of Aβ and tau into the ISF from synaptic-metabolic
962 activity, k_{cell_rel}, decreases with sleep but remains time-invariant during sleep. In this model,
963 morning plasma levels of Aβ and tau species are assumed not to be influenced by either of the
964 two groups (***Physio***, ***Hypno***) of sleep-related predictors. Letting $\boldsymbol{Conc_{AM}}$ and $\boldsymbol{Conc_{PM}}$ denote the
965 morning and evening plasma levels of the five Aβ and tau biomarkers $A\beta_{40}$, $A\beta_{42}$, np-tau181, np-
966 tau217 and p-tau181, respectively, the **null model** is the multivariate linear mixed model that
967 regresses $\boldsymbol{Conc_{AM}}$ on $\boldsymbol{Comc_{PM}}$ with covariates of amyloid status, age, APOE-ε4 status, sex,
968 circadian rhythm and study site, with participant ID as random intercept. This multivariate model
969 was solved using R library lme4 after transforming the $\boldsymbol{Conc_{AM}}$ and $\boldsymbol{Conc_{PM}}$ into one-
970 dimensional vectors and adding a variable *biomarker* to index these observations in the original
971 data[69]. The categorical *biomarker* variable was included in the model as an interaction term with
972 the transformed $\boldsymbol{Conc_{PM}}$ and as a vector of random slopes. Specifically, random effects were
973 specified as (biomarker - 1 | id) in **lme4** syntax, yielding a full (unstructured) covariance matrix
974 among the five biomarker-specific slopes. This formulation allowed correlations between
975 biomarker variables to be estimated via their shared subject-level covariance structure,
976 effectively modeling cross-biomarker dependencies within participants. $\boldsymbol{Conc_{AM}}$ and $\boldsymbol{Conc_{PM}}$
977 were rescaled to improve numerical stability of the linear mixed model estimation. Specifically,
978 values for $A\beta_{40}$ were divided by 10 so that regression coefficients reflect the effect of a 10-unit
979 increase in the original scale.
980
981 The **neuro-glymphatic model** represented the alternative hypothesis that clearance of Aβ and
982 tau species from the ISF to plasma is dependent on (i) sleep-active glymphatic exchange, with
983 k_{glymph_out} and k_{glymph_in} increasing overnight in the sleep condition; and (ii) variation in

synaptic-metabolic Aβ and tau species release into the ISF through overnight changes in k_{cell_rel}. Three glymphatic models were tested, two for the sleep condition with the first, ***Physio$_S$***, using features of parenchymal resistance, sleep neurophysiology, central noradrenergic tone, and cerebrovascular function while the second, ***Hypno$_S$***, reflects only hypnographic sleep stage duration. For the sleep deprivation/wake condition, ***Physio$_W$***, used the same features as ***Physio$_S$***. The predictors ***Physio$_S$*** and ***Physio$_W$*** denote single predictors constructed from the linear combination of R_p, HRV, PTT, and EEG power bands during the sleep and sleep deprivation (wake) conditions, respectively. The predictor ***Hypno$_S$*** denotes the single predictor constructed from the linear combination of REM, NREM, N1 and WASO hypnogram stage duration. The two sleep **neuro-glymphatic models** added to the **null model** the predictors ***Physio$_S$*** and ***Hypno$_S$*** and their respective interaction terms with evening levels of plasma Aβ and tau ***Physio$_S$*** * ***Conc$_{PM}$*** and ***Hypno$_S$*** * ***Conc$_{PM}$***. The sleep deprivation/wake **neuro-glymphatic model** added to the **null model** the predictor ***Physio$_W$*** and the interaction term ***Physio$_W$*** * ***Conc$_{PM}$***. The R *Anova* function in the car package was used for analysis of deviance using a Type III Wald Chi-square test for the interaction effects.

The likelihood ratio test (LRT) was used for significance testing of the **neuro-glymphatic model** versus the **null model**. Of particular interest was the percent of the residual variation in the **null model** that was explained by the **glymphatic model**; that is, the additional variation explained by including one of the single predictors ***Physio$_S$***, ***Physio$_W$*** or ***Hypno$_S$*** in the **neuro-glymphatic model** under the normal sleep or sleep deprivation/wake conditions. The residual variation of each model was computed from the sum of the square difference between the observed morning plasma AD biomarker levels and the fitted morning plasma levels for $A\beta_{40}$, $A\beta_{42}$, np-tau181, np-tau217 and p-tau181 individually using maximum likelihood and conditional on the random effects. Letting RSS_0 and RSS denote these two quantities for the **null model** and a

1009 **glymphatic model**, $1 - \frac{RSS}{RSS_0}$ gives the R^2 of the multivariate linear mixed models[67]. Confidence
1010 intervals for these R^2 estimates were computed from quantiles on 1,000 conditional parametric
1011 bootstrap resamples.
1012
1013 *Sensitivity analysis to define individual predictor contributions*
1014 We quantified the contribution of each individual predictor to glymphatic clearance or synaptic-
1015 metabolic release during sleep by simulating changes in the magnitude of $\boldsymbol{Physio_S}$. A sensitivity
1016 analysis of the individual predictors within $\boldsymbol{Physio_S}$ was conducted using the **neuro-glymphatic**
1017 **model** (**Table 5**). Morning plasma concentrations of AD biomarkers $\boldsymbol{Conc_{AM}}$ were simulated
1018 following a 5% increase in the magnitude of each predictor (**Supplemental Table 8**). By
1019 multiplying the effect of each predictor by its respective weight in the linear single-predictor
1020 $\boldsymbol{Physio_S}$, we determined that a negative value indicated that a **decrease** in predictor magnitude
1021 led to an **increase** in $\boldsymbol{Conc_{AM}}$, whereas a positive value indicated that an **increase** in predictor
1022 magnitude resulted in a **decrease** in $\boldsymbol{Conc_{AM}}$ (**Supplemental Table 8**). Notably, a decrease in
1023 $\boldsymbol{Physio_S}$ led to all individual predictors increasing morning plasma concentrations of AD
1024 biomarkers.
1025
1026 To define if this increase in morning plasma AD biomarker levels was attributable to enhanced
1027 glymphatic clearance or from increased synaptic-metabolic release, we referenced the
1028 numerical sign (+/-) of the individual predictor weights in $\boldsymbol{Physio_s}$, with (i) a positive sign (+)
1029 reflecting that a *decrease* in that predictor contributes to the increase in morning plasma AD
1030 biomarker concentrations, and (ii) a negative sign (-) reflecting that an *increase* in that predictor
1031 contributes to the increase in morning plasma AD biomarker concentrations. For each of these
1032 individual predictors, their presumed effect upon glymphatic clearance and synaptic-metabolic
1033 release of Aβ and tau can be defined based on prior literature[12,13,16,17,22,23,25,29-31,40,41,70-73], as outlined in

1034 **Supplemental Table 9**. By combining the numerical signs of the individual predictor weights
1035 and the individual predictor's presumed effects on glymphatic clearance and synaptic-metabolic
1036 release of Aβ and tau, the likely mechanism linking the individual predictor to the increase in
1037 morning plasma AD biomarker levels could be inferred (**Supplemental Table 8**, right column).
1038
1039 As an example, **Supplemental Table 8** shows that the effect of PTT is to increase $\boldsymbol{Conc_{AM}}$
1040 when $\boldsymbol{Physio_S}$ is decreased, an effect that could be attributable to an increase in brain-to-blood
1041 clearance, or increased synaptic-metabolic release of Aβ and tau. Because the numerical sign
1042 of the PTT weight estimate is negative (-0.034 for amyloid-positive individuals), its magnitude
1043 increases when $\boldsymbol{Physio_S}$ is decreased. Combining these two results, the effect of an *increase* in
1044 PTT is to *increase* $\boldsymbol{Conc_{AM}}$. Based on the role that vasomotor oscillations play in perivascular
1045 transport and glymphatic clearance[12,13,25,40], it is presumed that this effect of PTT on $\boldsymbol{Conc_{AM}}$
1046 occurs through enhanced clearance by increasing perivascular CSF transport. Using a similar
1047 approach, we conclude that sleep-related individual predictors that are associated with
1048 increased glymphatic function, such as NREM EEG delta power[13,17,22,23], cerebrovascular
1049 compliance measured by PTT[12,13,25,40], and R_P[13,17] were each associated with increased
1050 overnight clearance of Aβ and tau into the plasma. In contrast, NREM EEG theta and REM EEG
1051 theta and beta spectral power appear to be linked to elevated production[29-31,73].
1052
1053 The compartmental pharmacokinetic model predicts that increases in both sleep-active
1054 glymphatic function and synaptic-metabolic activity contribute to increased morning plasma AD
1055 biomarker levels (**Figure 1A–B**). Consistent with this prediction, as shown in **Supplemental**
1056 **Table 8**, at the mean evening plasma biomarker values, a decrease in overnight $\boldsymbol{Physio_S}$
1057 corresponded to higher morning plasma AD biomarker levels across all individual predictors.
1058 Because each neurophysiologic predictor in $\boldsymbol{Physio_S}$ was normalized to its value at sleep

1059 onset[17], its weight in the linear combination defining ***Physio$_S$*** reflects its relative contribution to
1060 its primary mechanism driving morning biomarker increases. As evident from **Table 4** and
1061 **Supplemental Table 8**, parenchymal resistance R_P, which is a key determinant of sleep-active
1062 glymphatic clearance[13,17], was the dominant contributor to ***Physio$_S$***, while other
1063 neurophysiological predictors (PTT, HRV, EEG power bands) had comparatively minor effects
1064 on either glymphatic clearance or synaptic-metabolic release.
1065
1066
1067

1068 **Supplemental Table 1. Effect of changes in glymphatic clearance or Aβ and tau release**
1069 **on plasma Aβ42/Aβ40 and p-tau/np-tau ratios.**
1070

$k_{on-rate}$	$k_{off-rate}$	Change in k_{glymph_in} and k_{glymph_out}	Change in k_{cell_rel}	Increase in Aβ42/ Aβ40	Increase in p-tau/np-tau
0	-	*Any*	*Any*	0%	0%
7.2 hr^{-1}	0.32 hr^{-1}	*2.0x*	-	4.7%	4.9%
7.2 hr^{-1}	0.32 hr^{-1}	-	*0.5x*	7.4%	4.4%
1.0 hr^{-1}	0.1 hr^{-1}	*2.0x*	-	3.4%	3.5%
1.0 hr^{-1}	0.1 hr^{-1}	-	*0.5x*	5.1%	2.5%
1.0 hr^{-1}	1.0 hr^{-1}	*2.0x*	-	2.4%	2.6%
1.0 hr^{-1}	1.0 hr^{-1}	-	*0.5x*	4.0%	2.5%
0.1 hr^{-1}	1.0 hr^{-1}	*2.0x*	-	0.4%	0.4%
0.1 hr^{-1}	1.0 hr^{-1}	-	*0.5x*	0.7%	0.5%
7.2 hr^{-1}	0.32 hr^{-1}	*0.5x*	-	-2.5%	-2.4%
7.2 hr^{-1}	0.32 hr^{-1}	-	*1.5x**	-4.9%	-3.1%
1.0 hr^{-1}	0.1 hr^{-1}	*0.5x*	-	-1.7%	-1.6%
1.0 hr^{-1}	0.1 hr^{-1}	-	*1.5x*	-3.4%	-1.9%
1.0 hr^{-1}	1.0 hr^{-1}	*0.5x*	-	-1.4%	-1.3%
1.0 hr^{-1}	1.0 hr^{-1}	-	*1.5x*	-2.6%	-1.8%
0.1 hr^{-1}	1.0 hr^{-1}	*0.5x*	-	-0.2%	-0.2%
0.1 hr^{-1}	1.0 hr^{-1}	-	*1.5x*	-0.5%	-0.3%

1071 *A 1.5x increase in $k_{cell_{rel}}$ during sleep put it at 105% of its value at wake.

1072

1073 **Supplemental Table 2: Cerebrovascular and peripheral PTT during sleep and wake visits.**

1074

Amyloid Status	PTT	Sleep	DF	Wake	DF	P
Positive	cerebrovascular	1.08 (0.42)	11	1.26 (0.51)	9	0.417
	peripheral	1.16 (0.66)	11	1.35 (0.46)	9	0.463
Negative	cerebrovascular	1.24 (0.40)	14	1.22 (0.52)	12	0.915
	peripheral	1.47 (0.90)	14	1.09 (0.24)	12	0.146

1075 *Data shown as mean (SD). PTT, pulse transit time; DF, degrees of freedom; P, p-value.

Supplemental Table 3: Prediction of morning CBV for gray and white matter ROI following overnight sleep with NREM cerebrovascular PTT *(prediction model)* and without *(null model)* in amyloid positive and amyloid negative individuals*.

Model	Predictor Group	Predictor		Amyloid Positive				Amyloid Negative			
				Estimate	DF	CI	P	Estimate	DF	CI	P
Null Model	Fixed Effects	Age		0.289	46	0.287– 0.292	**<0.001**	-0.008	70	-0.023 – 0.007	0.313
		Sex (male)		-0.427	46	-0.438 – -0.417	**<0.001**	0.488	70	0.381 – 0.596	**<0.001**
		APOE-ε4 (positive)		1.501	46	1.489 – 1.512	**<0.001**	-0.398	70	-0.519 – -0.278	**0.047**
		Circadian		-0.033	46	-0.033 – -0.032	**<0.001**	0.000	70	-0.001 – -0.000	0.343
	Random Effects	σ^2		0				0.001			
		$\tau_{11\ pid.Frontal\ GM}$		0.745				4.028			
		$\tau_{11\ pid.Frontal\ WM}$		2.636				0.275			
		$\tau_{11\ pid.Occipital\ GM}$		29.092				79.264			
		$\tau_{11\ pid.Occipital\ WM}$		3.55				0.564			
		$\tau_{11\ pid.Parietal\ GM}$		2.895				15.981			
		$\tau_{11\ pid.Parietal\ WM}$		2.539				0.146			
		$\tau_{11\ pid.Temporal\ GM}$		5.276				20.111			
		$\tau_{11\ pid.Temporal\ WM}$		2.415				0.275			
Prediction Model	Fixed Effects	Age		0.27	38	0.269 – 0.271	**<0.001**	-0.021	62	-0.025 – -0.016	**<0.001**
		Sex (male)		-0.304	38	-0.308 – -0.3	**<0.001**	0.218	62	0.179 – 0.256	**<0.001**
		APOE-ε4 (positive)		1.345	38	1.341 – 1.35	**<0.001**	-0.385	62	-0.425 – -0.346	**<0.001**
		Circadian		-0.032	38	-0.032 – -0.032	**<0.001**	-0.001	62	-0.002 – -0.001	**<0.001**
		Predictor Effects	0.157	0.970	38	-0.25 – 0.564	0.463	2.046	62	1.556 – 2.536	**<0.001**
			-1.328	-0.516	38	-1.792 – -0.864	**<0.001**	0.489	62	0.296 – 0.682	**<0.001**
			5.151	5.964	38	3.513 – 6.789	**<0.001**	6.991	62	5.311 – 8.671	**<0.001**
			-1.589	-0.776	38	-2.112 – -1.066	**<0.001**	0.383	62	0.12 – 0.646	**0.012**
			1.612	2.424	38	1.058 – 2.166	**<0.001**	3.489	62	2.671 – 4.308	**<0.001**
			-1.382	-0.570	38	-1.795 – -0.97	**<0.001**	0.526	62	0.378 – 0.674	**<0.001**
			2.128	2.941	38	1.363 – 2.894	**<0.001**	3.849	62	2.953 – 4.745	**<0.001**
			-1.201	-0.388	38	-1.684 – -0.718	**<0.001**	0.634	62	0.366 – 0.902	**<0.001**
	Random Effects	σ^2		0				0.000			
		$\tau_{11\ pid.Frontal\ GM}$		0.655				1.444			
		$\tau_{11\ pid.Frontal\ WM}$		0.85				0.215			
		$\tau_{11\ pid.Occipital\ GM}$		10.589				17.078			
		$\tau_{11\ pid.Occipital\ WM}$		1.079				0.408			
		$\tau_{11\ pid.Parietal\ GM}$		1.211				4.048			
		$\tau_{11\ pid.Parietal\ WM}$		0.671				0.122			
		$\tau_{11\ pid.Temporal\ GM}$		2.311				4.851			
		$\tau_{11\ pid.Temporal\ WM}$		0.919				0.425			

*CBV, cerebral blood volume; ROI, region of interest; GM, gray matter; WM, white matter; DF, degrees of freedom; CI, 95% confidence interval; P, p-value; PTT, cerebrovascular pulse-transit time measured during NREM sleep; σ^2, residual variance; τ_{11}, random slope variance; **Bolded P values reflect significant associations at P < 0.05**. Shaded cells demark random effects and potential biological confounders.

Supplemental Table 4: Prediction of morning CBV for gray and white matter ROI following overnight sleep deprivation (wake) with cerebrovascular PTT *(prediction model)* and without *(null model)* in amyloid positive and amyloid negative individuals*.

Model	Predictor Group	Predictor		Amyloid Positive				Amyloid Negative			
				Estimate	DF	CI	P	Estimate	DF	CI	P
Null Model	Fixed Effects	Age		0.143	30	0.141 – 0.145	**<0.001**	-0.214	54	-0.218 – -0.211	**<0.001**
		Sex (male)		-1.549	30	-1.56 – -1.538	**<0.001**	-1.263	54	-1.285 – -1.241	**<0.001**
		APOE-ε4 (positive)		0.566	30	0.558 – 0.575	**<0.001**	-1.355	54	-1.382 – -1.327	**<0.001**
		Circadian		0.009	30	0.009 – 0.009	**<0.001**	0.015	54	0.015 – 0.015	**<0.001**
	Random Effects	σ^2		0				0.000			
		$\tau_{11\ pid.Frontal\ GM}$		8.214				27.216			
		$\tau_{11\ pid.Frontal\ WM}$		1.998				13.874			
		$\tau_{11\ pid.Occipital\ GM}$		54.045				96.675			
		$\tau_{11\ pid.Occipital\ WM}$		10.197				13.704			
		$\tau_{11\ pid.Parietal\ GM}$		18.142				40.641			
		$\tau_{11\ pid.Parietal\ WM}$		5.906				14.008			
		$\tau_{11\ pid.Temporal\ GM}$		23.893				52.848			
		$\tau_{11\ pid.Temporal\ WM}$		5.129				15.828			
Prediction Model	Fixed Effects	Age		0.264	22	0.264 – 0.264	**<0.001**	0.003	46	-0.002 – 0.009	0.262
		Sex (male)		0.382	22	0.381– 0.383	**<0.001**	-0.525	46	-0.561 – -0.49	**<0.000**
		APOE-ε4 (positive)		3.022	22	3.020 – 3.023	**<0.001**	-0.344	46	-0.387 – -0.301	**<0.000**
		Circadian		0.000	22	0.000 – 0.000	**<0.001**	-0.001	46	-0.001 – 0.000	**0.016**
		Predictor Effects	Frontal GM: PTT	3.178	22	2.713 – 3.643	**<0.001**	2.17	46	1.551 – 2.789	**<0.000**
			Frontal WM: PTT	1.834	22	1.325 – 2.343	**<0.001**	0.765	46	0.487 – 1.043	**0.002**
			Occipital GM: PTT	7.165	22	5.833 – 8.497	**<0.001**	6.334	46	4.514 – 8.154	**<0.000**
			Occipital WM: PTT	2.253	22	1.087 – 3.418	**0.002**	0.716	46	0.449 – 0.982	**0.003**
			Parietal GM: PTT	4.39	22	3.977 – 4.803	**<0.001**	3.246	46	2.381 – 4.111	**<0.000**
			Parietal WM: PTT	2.379	22	1.65 – 3.107	**<0.001**	0.822	46	0.594 – 1.049	**0.001**
			Temporal GM: PTT	4.913	22	4.01 – 5.817	**<0.001**	4.09	46	3.018 – 5.162	**<0.000**
			Temporal WM: PTT	2.221	22	1.472– 2.97	**<0.001**	1.065	46	0.787 – 1.344	**<0.000**
	Random Effects	σ^2		0.000				0.000			
		$\tau_{11\ pid.Frontal\ GM}$		0.920				2.063			
		$\tau_{11\ pid.Frontal\ WM}$		1.100				0.414			
		$\tau_{11\ pid.Occipital\ GM}$		7.539				17.889			
		$\tau_{11\ pid.Occipital\ WM}$		5.773				0.379			
		$\tau_{11\ pid.Parietal\ GM}$		0.724				4.04			
		$\tau_{11\ pid.Parietal\ WM}$		2.253				0.275			
		$\tau_{11\ pid.Temporal\ GM}$		3.466				6.201			
		$\tau_{11\ pid.Temporal\ WM}$		2.382				0.414			

*CBV, cerebral blood volume; ROI, region of interest; GM, gray matter; WM, white matter; DF, degrees of freedom; CI, 95% confidence interval; P, p-value; PTT, cerebrovascular pulse-transit time measured during NREM sleep; σ^2, residual variance; τ_{11}, random slope variance; **Bolded P values reflect significant associations at P < 0.05**. Shaded cells demark random effects and potential biological confounders.

Supplemental Table 5: Likelihood ratio test of the *prediction model* versus the *null model.**

Condition	Amyloid Status	Model	AIC	BIC	logLik	LRT	DF	P
Sleep Condition	**Positive**	Null	117.9	221.9	-16.9			
		Prediction	81.3	205.2	9.3	52.5	8	**<0.001**
	Negative	Null	247.9	362.1	-81.9			
		Prediction	202.8	338.7	-51.4	61.1	8	**<0.001**
Sleep Deprivation/Wake	**Positive**	Null	166.7	262.4	-41.4			
		Prediction	113.9	227.7	-7.0	68.8	8	**<0.001**
	Negative	Null	153.3	261.0	-34.6			
		Prediction	149.0	277.2	-24.5	20.3	8	**0.009**

*AIC, Akaike Information Criteria; BIC, Bayesian Information Criteria; logLik, log likelihood; LRT, log likelihood ratio; DF, degrees of freedom; P, p-value; **Bolded P values reflect significant LRT at P < 0.05**.

Supplemental Table 6. Percent of variance in morning plasma AD biomarker levels explained by the *neuro-glymphatic model* over the *null model.**

Condition	Amyloid Status	ROI	Variance Explained (%)	CI
Sleep Condition	Positive	**All**	**66.8**	**57.9 – 90.0**
		Frontal GM	7.2	-166.8 – 81.0
		Frontal WM	**73.2**	**26.0 – 94.7**
		Parietal GM	**65.3**	**38.9 – 94.4**
		Parietal WM	**77.9**	**34.2 – 95.9**
		Occipital GM	**66.4**	**56.1 – 93.4**
		Occipital WM	**75.4**	**38.9 – 95.0**
		Temporal GM	**61.5**	**41.4 – 93.3**
		Temporal WM	**68.1**	**15.8 – 93.5**
	Negative	**All**	**76.8**	**66.3 – 92.1**
		Frontal GM	**64.9**	**53.6 – 93.4**
		Frontal WM	23.0	-21.8 – 88.9
		Parietal GM	**75.2**	**63.4 – 93.5**
		Parietal WM	17.6	-15.8 – 92.8
		Occipital GM	**78.9**	**65.9 – 93.4**
		Occipital WM	28.4	-34.0 – 78.3
		Temporal GM	**76.5**	**64.5 – 93.5**
		Temporal WM	-54.6	-12.6 – 84.1
Sleep Deprivation/Wake	Positive	**All**	**84.6**	**56.5 – 94.9**
		Frontal GM	91.8	-60.1 – 98.8
		Frontal WM	60.1	-69.1 – 98.1
		Parietal GM	**97.1**	**34.6 – 99.1**
		Parietal WM	70.1	-71.4 – 95.4
		Occipital GM	**88.9**	**43.2 – 97.4**
		Occipital WM	43.2	-56.4 – 91.3
		Temporal GM	**88.0**	**9.7 – 97.2**
		Temporal WM	60.7	-41.0 – 96.8
	Negative	**All**	**93.5**	**65.1 – 92.7**
		Frontal GM	**95.7**	**61.5 – 93.6**
		Frontal WM	**98.3**	**38.9 – 92.3**
		Parietal GM	**94.4**	**66.1 – 94.1**
		Parietal WM	**98.9**	**58.1 – 95.2**
		Occipital GM	**89.6**	**62.0 – 93.1**
		Occipital WM	**98.4**	**35.2 – 91.9**
		Temporal GM	**93.4**	**67.7 – 94.4**
		Temporal WM	**98.5**	**64.7 – 95.1**

*ROI, region of interest; GM, gray matter; WM, white matter; CI, 95% confidence interval.
Bolded CI values reflect significant values using quantile bootstrapping.

Supplemental Table 7. Estimate for single predictor coefficient in the *neuro-glymphatic model* in sleep and sleep deprivation evaluated at the mean evening plasma AD biomarker levels*.

Condition and Predictor	Amyloid Status	Factor	Estimate at Mean Value of $Conc_{PM}$ for Biomarker	P of Main Effect	P of Interaction Effect
Sleep Condition $Physio_S$	Positive	$(1+\overline{Conc}_{PM,Ab40})\ Physio_S$	-327.245	**0.035**	**<0.001**
		$(1+\overline{Conc}_{PM,Ab42})\ Physio_S$	-297.768	**0.030**	**<0.001**
		$(1+\overline{Conc}_{PM,Tau})\ Physio_S$	-442.340	**0.015**	**<0.001**
	Negative	$(1+\overline{Conc}_{PM,Ab40})\ Physio_S$	-5.733	0.179	**0.017**
		$(1+\overline{Conc}_{PM,Ab42})\ Physio_S$	-7.652	**0.001**	**<0.001**
		$(1+\overline{Conc}_{PM,nTau181})\ Physio_S$	-7.179	**<0.001**	**<0.001**
		$(1+\overline{Conc}_{PM,nTau217})\ Physio_S$	-6.619	**<0.001**	**<0.001**
		$(1+\overline{Conc}_{PM,pTau181})\ Physio_S$	-3.607	0.206	**<0.001**
Sleep Condition $Hypno_S$	Positive	$(1+\overline{Conc}_{PM,Ab40})\ Hypno_S$	-0.137	**0.015**	**0.025**
		$(1+\overline{Conc}_{PM,Ab42})\ Hypno_S$	-0.134	**0.023**	0.057
		$(1+\overline{Conc}_{PM,Tau})\ Hypno_S$	0.075	0.184	**0.041**
	Negative	$(1+\overline{Conc}_{PM,Ab40})\ Hypno_S$	-0.038	**0.001**	**0.001**
		$(1+\overline{Conc}_{PM,Ab42})\ Hypno_S$	-0.070	**<0.001**	**<0.001**
		$(1+\overline{Conc}_{PM,nTau181})\ Hypno_S$	-0.058	**<0.001**	**<0.001**
		$(1+\overline{Conc}_{PM,nTau217})\ Hypno_S$	-0.050	**<0.001**	**<0.001**
		$(1+\overline{Conc}_{PM,pTau181})\ Hypno_S$	0.003	**<0.001**	**<0.001**
Sleep Deprivation/Wake $Physio_W$	Positive	$(1+\overline{Conc}_{PM,Ab40})\ Physio_W$	4.746	0.290	0.281
		$(1+\overline{Conc}_{PM,Ab42})\ Physio_W$	5.725	0.313	0.318
		$(1+\overline{Conc}_{PM,Tau})\ Physio_W$	-51.708	0.433	**<0.001**
	Negative	$(1+\overline{Conc}_{PM,Ab40})\ Physio_W$	-9.636	**<0.001**	**0.002**
		$(1+\overline{Conc}_{PM,Ab42})\ Physio_W$	-9.682	**<0.001**	**0.001**
		$(1+\overline{Conc}_{PM,nTau181})\ Physio_W$	-4.140	**<0.001**	**<0.001**
		$(1+\overline{Conc}_{PM,nTau217})\ Physio_W$	-4.158	**<0.001**	**<0.001**
		$(1+\overline{Conc}_{PM,pTau181})\ Physio_W$	-3.393	**<0.001**	**<0.001**

$Conc_{PM}$, evening plasma level for the biomarker; ***$Physio_S$*** and ***$Physio_W$***, single predictors constructed from the linear combination of the full model predictors during the sleep and sleep deprivation (wake) conditions, respectively, for both amyloid positive and negative participants separately; ***$Hypno_S$***, single predictor constructed from the full model hypnogram features during the sleep condition for both amyloid positive and negative participants separately; **Bolded P values reflect significant LRT at P < 0.05**.

Supplemental Table 8. Change in morning plasma levels of AD biomarker levels under sleep and sleep deprivation conditions following a 5% magnitude increase in a predictor*.

Condition and Predictor	Amyloid Status	Predictors	Estimate	Effect on $Conc_{AM}$ at Mean Value of $Conc_{PM}$ Following a 5% Magnitude Increase in Predictor					Individual Predictor Effect on $Conc_{AM}$ when $Physio_S$, $Hypno_S$, or $Physio_W$ are Decreased	Increased Clearance or Increased Production Mechanism
				$A\beta 40$	$A\beta 42$	$nTau181$	$nTau217$	$pTau181$		
						$Tau\ Aggregate$				
Sleep Condition *$Physio_S$*	**Positive**	R_p	0.968	-14.589	-13.275		-19.720		Increase	Clearance
		PTT (NREM)	-0.034	0.607	0.553		0.821		Increase	Clearance
		HRV (NREM)	-0.068	1.581	1.439		2.138		Increase	Clearance
		EEG Delta Power (NREM)	0.086	-1.915	-1.743		-2.589		Increase	Production
		EEG Theta Power (NREM)	0.162	-2.585	-2.352		-3.494		Increase	Production
		EEG Theta Power (REM)	-0.146	2.467	2.245		3.335		Increase	Clearance
		EEG Beta Power (REM)	-0.041	0.806	0.734		1.090		Increase	Production
	Negative	R_p	0.963	-0.255	-0.341	-0.320	-0.295	-0.161	Increase	Clearance
		PTT (NREM)	-0.058	0.019	0.025	0.024	0.022	0.012	Increase	Clearance
		HRV (NREM)	0.114	-0.043	-0.058	-0.054	-0.050	-0.027	Increase	Production
		EEG Delta Power (NREM)	-0.041	0.014	0.019	0.018	0.017	0.009	Increase	Clearance
		EEG Theta Power (NREM)	0.169	-0.044	-0.059	-0.056	-0.051	-0.028	Increase	Production
		EEG Theta Power (REM)	0.087	-0.027	-0.036	-0.034	-0.031	-0.017	Increase	Production
		EEG Beta Power (REM)	-0.135	0.072	0.096	0.090	0.083	0.045	Increase	Production
Sleep Condition *$Hypno_S$*	**Positive**	NREM Duration	-0.182	0.263	0.257		-0.143		Increase	Clearance
		REM Duration	-0.519	0.204	0.200		-0.111		Increase	Production
		N1 Duration	0.834	-0.267	-0.262		0.145		Increase	Clearance
		WASO Duration	0.044	-0.022	-0.021		0.012		Increase	Clearance
	Negative	NREM Duration	-0.090	0.032	0.059	0.049	0.042	-0.003	Increase	Clearance
		REM Duration	0.525	-0.069	-0.128	-0.106	-0.092	0.006	Increase	Clearance
		N1 Duration	0.801	-0.076	-0.141	-0.116	-0.101	0.007	Increase	Clearance
		WASO Duration	0.273	-0.019	-0.036	-0.030	-0.026	0.002	Increase	Clearance
Sleep Deprivation/ Wake *$Physio_W$*	**Positive**	R_p	0.621	0.149	0.180		-1.624		Increase	Clearance
		PTT	0.190	0.054	0.065		-0.583		Increase	Production
		HRV	-0.242	-0.065	-0.079		0.712		Increase	Clearance
		EEG Delta Power	-0.487	-0.112	-0.135		1.223		Increase	Production
		EEG Theta Power	-0.382	-0.102	-0.124		1.116		Increase	Production
		EEG Beta Power	0.371	0.114	0.138		-1.246		Increase	Clearance
	Negative	R_p	0.626	-0.300	-0.301	-0.129	-0.129	-0.106	Increase	Clearance
		PTT	-0.004	0.002	0.002	0.001	0.001	0.001	Increase	Clearance
		HRV	0.136	-0.094	-0.094	-0.040	-0.041	-0.033	Increase	Production
		EEG Delta Power	-0.658	0.335	0.337	0.144	0.145	0.118	Increase	Production
		EEG Theta Power	-0.391	0.211	0.212	0.091	0.091	0.074	Increase	Production
		EEG Beta Power	0.062	-0.032	-0.032	-0.014	-0.014	-0.011	Increase	Clearance

*R_p, Parenchymal Resistance; PTT, Pulse Transit Time; HRV, Heart Rate Variability; EEG, Electroencephalography; ***$Physio_S$*** and ***$Hypno_S$***, single predictors for sleep and ***$Physio_W$*** single predictors for sleep deprivation.

Supplemental Table 9. Effects of increasing predictors in *Physio*$_S$ and *Hypno*$_S$ on sleep-dependent glymphatic clearance and synaptic-metabolic solute production.

Condition	Increased Predictor	Description	Effect on Glymphatic Clearance[12,13,16,17,22,23,25,40,41,70-72]	Effect on Release[29-31,73]
Sleep Condition *Physio*$_S$	**Rp**	Parenchymal resistance; reflects the ratio between intracellular and extracellular brain fluid.	Higher **Rp** indicates ISF shifting into astrocytes, narrowing the interstitial space and reducing glymphatic flow → **decreased clearance**.	**None expected.**
	PTT (NREM)	Pulse transit time during NREM; indexes arterial wall compliance - greater compliance strengthens the CSF driving force along perivascular spaces (PVS).	**Increased PTT** in NREM → **increased clearance**.	**None expected.**
	HRV (NREM)	Heart-rate variability during NREM; rises as peripheral sympathetic tone falls relative to vagal tone.	**Increased HRV** from reduced sympathetic tone (low LC activity) is expected to **increase clearance**.	**Increased HRV** from reduced sympathetic tone (low LC activity) is expected to **decrease production**.
	EEG Delta Power (NREM)	Generated by cortical pyramidal and corticothalamic loops; alternating UP states (mass depolarization, strong EPSCs/IPSCs) and DOWN states (hyperpolarization).	**Higher delta power** indicates stronger synchronized oscillations → **increased clearance**.	**Higher delta power** reflects long quiescent hyperpolarization → **decreased production**.
	EEG Theta Power (NREM)	Generated by hippocampal–septal and limbic–cortical coupling; carries the second-largest summed synaptic current in NREM. Aligns with NREM microarousals	**Higher theta power** indicates more synchronized oscillations → **increased clearance**.	A **relative increase in theta** at the expense of delta shifts low frequency to higher frequency postsynaptic currents → **increased production**. A **relative increase in theta** at the expense of other band powers shifts from higher frequency to low frequency postsynaptic currents → **decreased production**.
	EEG Theta Power (REM)	Generated by hippocampal CA1–CA3 loops with rhythmic EPSCs/IPSCs in hippocampal pyramids and entorhinal cortex; phase-locked interneuron firing; largest summed postsynaptic currents in REM.	**Higher theta power** → more synchrony → **increased clearance**.	**Higher theta power** → larger summed postsynaptic currents → **increased production**.
	EEG Beta Power (REM)	Generated by cortical pyramidal–interneuron loops; activity is largely asynchronous.	**Increase** is not expected to increase synchrony → **no change in clearance**.	**Higher beta power** → larger summed high frequency postsynaptic currents → **increased production**.
Sleep Condition *Hypno*$_S$	**NREM Duration**	Duration of NREM (N2 and N3) sleep; surrogate for NREM physiology	↑ NREM sleep → ↑ NREM clearance duration	↑ NREM sleep → ↓ production
	REM Duration	Duration of REM sleep; surrogate for REM physiology	↑ REM sleep → ↑ REM clearance duration	↑ REM sleep → ↑ production
	N1 Duration	Duration of N1 sleep	None expected, or ↓ clearance if it replaces NREM or REM	↑ production relative to NREM
	WASO Duration	Duration of wake after sleep onset	↓ clearance relative to sleep	↑ production relative to sleep

Supplemental Table 10. Prediction of morning plasma AD biomarker levels following overnight sleep using the *null model* and the *neuro-glymphatic model* with *Hypnos.**

Model	Predictor Group	Predictor		Amyloid Positive				Amyloid Negative			
				Estimate	DF	CI	P	Estimate	DF	CI	P
Null Model	Fixed Effects	Age		-0.827	42	-1.856 – 0.203	0.113	0.075	108	-0.074 – 0.223	0.323
		Sex (male)		4.504	42	0.026 – 8.982	**0.049**	0.652	108	-0.587 – 1.890	0.299
		APOE-e4 (positive)		-2.148	42	-6.949 – 2.652	0.372	-1.077	108	-2.365 – 0.212	0.101
		Circadian		0.039	42	-0.055 – 0.133	0.411	0.003	108	-0.008 – 0.014	0.590
		Study (Villages)		-	-	-	-	-1.309	108	-2.986 – 0.367	0.124
		Evening Biomarker Effects	***Conc$_{PM}$***	0.929	42	0.882 – 0.976	**<0.001**	0.959	108	0.933 – 0.986	**<0.001**
	Random Effects	σ^2		37.327				3.842			
		$\tau_{11\ pid\ Ab40}$		1.398				0.000			
		$\tau_{11\ pid\ Ab42}$		1.289				18.558			
		$\tau_{11\ Aggregate}$	$\tau_{11\ pid\ np\text{-}tau181}$	34.643				193.466			
			$\tau_{11\ pid\ np\text{-}tau217}$					352.682			
			$\tau_{11\ pid\ p\text{-}tau181}$					1.482			
Sleep Model	Fixed Effects	Age		-1.327	36	-2.419 – -0.236	**0.019**	0.179	98	0.075 – 0.283	**0.001**
		Sex (male)		5.709	36	-0.611 – 12.028	0.075	0.801	98	-0.106 – 1.708	0.083
		APOE-e4 (positive)		-2.816	36	-7.200 – 1.569	0.201	-0.479	98	-1.482 – 0.524	0.345
		Circadian		0.047	36	-0.067 – 0.162	0.406	0.006	98	-0.002 – 0.013	0.158
		Study (Villages)		-	-	-	-	-0.694	98	-2.093 – 0.705	0.327
		Evening Biomarker Effects	***Conc$_{PM}$***	1.070	36	1.008 – 1.132	**<0.001**	1.063	98	0.993 – 1.133	**<0.001**
		Predictor Effects	Ab40: ***Hypnos$_S$***	-0.769	36	-1.386 – -0.152	**0.016**	0.180	98	0.078 – 0.282	**0.001**
			Ab42: ***Hypnos$_S$***	-0.831	36	-1.550 – -0.113	**0.025**	0.390	98	0.244 – 0.537	**<0.001**
			np-tau181: ***Hypnos$_S$***	-0.267	36	-0.520 – -0.013	**0.040**	0.502	98	0.397 – 0.607	**<0.001**
			np-tau217: **Hypnos$_S$**		36			0.674	98	0.506 – 0.842	**<0.001**
			p-tau181: ***Hypnos$_S$***		36			0.079	98	0.050 – 0.108	**<0.001**
		Evening Biomarker: Predictor Interactions	(Ab40: ***Hypnos$_S$***) ***Conc$_{PM}$***	0.015	36	0.002 – 0.029	**0.026**	-0.005	98	-0.01 – -0.002	**<0.001**
			(Ab42: ***Hypnos$_S$***) ***Conc$_{PM}$***	0.021	36	-0.001 – 0.043	0.059	-0.010	98	-0.01 – -0.007	**<0.001**
			(np-tau181: ***Hypnos$_S$***) ***Conc$_{PM}$***	0.005	36	0.003 – 0.007	**<0.001**	-0.008	98	-0.01 – -0.006	**<0.001**
			np-tau217 ***Hypnos$_S$***) ***Conc$_{PM}$***					-0.009	98	-0.01 – -0.007	**<0.001**
			(p-tau181: ***Hypnos$_S$***) ***Conc$_{PM}$***					-0.007	98	-0.01 – -0.005	**<0.001**
	Random Effects	σ^2		21.942				0.798			
		$\tau_{11\ pid\ Ab40}$		0.026				7.210			
		$\tau_{11\ pid\ Ab42}$		0.472				21.417			
		$\tau_{11\ Aggregate}$	$\tau_{11\ pid\ np\text{-}tau181}$	28.280				58.270			
			$\tau_{11\ pid\ np\text{-}tau217}$					143.690			
			$\tau_{11\ pid\ p\text{-}tau181}$					0.374			

*DF, degrees of freedom; CI, 95% confidence interval; P, p-value; ***Hypnos$_S$***, single predictor constructed from the linear combination of EEG hypnogram sleep durations; ***Conc$_{PM}$***, evening plasma level; UF, University of Florida study site; EEG, Electroencephalography; R_P, Parenchymal Resistance; σ^2, residual variance; τ_{11}, random slope variance; **Bolded P values reflect significant associations at P < 0.05**. Shaded cells demark random effects and potential biological confounders.

Supplemental Table 11. Prediction of morning plasma Aβ and tau levels following overnight sleep using the *null model* and the *neuro-glymphatic model* with *Physio$_w$.**

Model	Predictor Group	Predictor		Amyloid Positive				Amyloid Negative			
				Estimate	DF	CI	P	Estimate	DF	CI	P
Null Model	Fixed Effects	Age		0.247	32	-1.756 – 2.251	0.803	0.213	92	0.008 – 0.419	**0.042**
		Sex (male)		0.872	32	-6.180 – 7.924	0.803	-0.052	92	-1.356 – 1.252	0.937
		APOE-e4 (positive)		1.768	32	-3.978 – 7.515	0.535	1.294	92	-0.310 – 2.898	0.113
		Circadian		-0.017	32	-0.080 – 0.046	0.592	-0.003	92	-0.023 – 0.017	0.762
		Study (Villages)		-	-	-	-	-1.251	92	-3.500 – 0.999	0.272
		Evening Biomarker Effects	***Conc$_{PM}$***	0.776	32	0.726 – 0.827	**<0.001**	0.929	92	0.899 – 0.958	**<0.001**
	Random Effects	σ^2		40.611				3.172			
		$\tau_{11\ pid\ Ab40}$		0.000				6.114			
		$\tau_{11\ pid\ Ab42}$		2.911				2.644			
		$\tau_{11\ Aggregate}$	$\tau_{11\ pid\ np\text{-}tau181}$	75.220				132.350			
			$\tau_{11\ pid\ np\text{-}tau217}$					218.979			
			$\tau_{11\ pid\ p\text{-}tau181}$					1.654			
Sleep Model	Fixed Effects	Age		1.260	26	0.341 – 2.179	**0.009**	0.085	82	-0.032 – 0.202	0.154
		Sex (male)		2.664	26	-0.300 – 5.628	0.076	-0.221	82	-1.010 – 0.568	0.579
		APOE-e4 (positive)		2.896	26	0.287 – 5.505	**0.031**	1.234	82	0.303 – 2.166	**0.010**
		Circadian		-0.018	26	-0.044 – 0.009	0.179	-0.005	82	-0.017 – 0.006	0.348
		Study (Villages)		-	-	-	-	-1.462	82	-2.74 – -0.181	**0.026**
		Evening Biomarker Effects	***Conc$_{PM}$***	0.983	26	0.935 – 1.031	**<0.001**	0.901	82	0.875 – 0.927	**<0.001**
		Predictor Effects	Ab40: Physio$_w$	40.932	26	-37.080 – 118.943	0.291	-50.963	82	-75.12 – -26.8	**<0.001**
			Ab42: Physio$_w$	48.893	26	-46.038 – 143.824	0.299	-45.050	82	-64.42 – -25.7	**<0.001**
			np-tau181: Physio$_w$	4.983	26	-7.942 – 17.908	0.435	-68.196	82	-99.04 – -37.4	**<0.001**
			np-tau217: Physio$_w$		26			-142.099	82	-174– -109.95	**<0.001**
			p-tau181: Physio$_w$		26			-18.129	82	-24.3 – -11.98	**<0.001**
		Evening Biomarker: Predictor Interactions	(Ab40: Physio$_w$) ***Conc$_{PM}$***	-0.839	26	-2.408 – 0.730	0.282	1.055	82	0.448 – 1.662	**0.001**
			(Ab42: Physio$_w$) ***Conc$_{PM}$***	-1.186	26	-3.513 – 1.142	0.305	0.860	82	0.420 – 1.299	**<0.001**
			(np-tau181: Physio$_w$) ***Conc$_{PM}$***	-0.729	26	-0.884 – -0.574	**<0.001**	1.003	82	0.583 – 1.423	**<0.001**
			np-tau217 Physio$_w$) ***Conc$_{PM}$***					1.742	82	1.404 – 2.079	**<0.001**
			(p-tau181: Physio$_w$) ***Conc$_{PM}$***					1.638	82	1.078 – 2.198	**<0.001**
	Random Effects	σ^2		11.517				0.750			
		$\tau_{11\ pid\ Ab40}$		0.631				4.203			
		$\tau_{11\ pid\ Ab42}$		4.231				3.561			
		$\tau_{11\ Aggregate}$	$\tau_{11\ pid\ np\text{-}tau181}$	1.447				127.261			
			$\tau_{11\ pid\ np\text{-}tau217}$					146.787			
			$\tau_{11\ pid\ p\text{-}tau181}$					2.467			

*DF, degrees of freedom; CI, 95% confidence interval; P, p-value; ***Physio$_w$***, single predictor constructed from the linear combination of parenchymal resistance R_P, cardio/cerebrovascular metrics and EEG powerbands; ***Conc$_{PM}$***, evening plasma level; UF, University of Florida study site; EEG, Electroencephalography; R_P, Parenchymal Resistance; σ^2, residual variance; τ_{11}, random slope variance; **Bolded P values reflect significant associations at P < 0.05**. Shaded cells demark random effects and potential biological confounders.

Supplemental Table 12. Effects of increasing predictors in *Physio$_W$* on glymphatic clearance and synaptic-metabolic solute production during sleep deprivation.

Condition	Increased Predictor	Description	Effect on Clearance	Effect on Production
Sleep Deprivation/Wake *Physio$_w$*	**R_p**	Parenchymal resistance during wake; reflects the ratio between intracellular and extracellular brain fluid.	Like sleep, higher **Rp** indicates ISF shifting into astrocytes, narrowing the interstitial space and reducing glymphatic flow → **decreased clearance**.	**None expected.**
	PTT	Pulse transit time during wake; indexes arterial wall compliance—greater compliance strengthens the CSF driving force along perivascular spaces (PVS).	Like sleep, **increased PTT** in NREM → **increased clearance**.	**None expected.**
	HRV	Heart-rate variability during wake; rises as peripheral sympathetic tone falls relative to vagal tone.	Like sleep, **increased HRV** from reduced sympathetic tone (low LC activity) is expected to **increase clearance**.	**Increased HRV** from reduced sympathetic tone (low LC activity) → **decreased production**.
	EEG Delta Power	Marker of local cortical network disengagement or dysregulation; low synchrony; increases with sleep pressure.	Sleep-like patches may disrupt glymphatic–vascular coupling, **reducing clearance.**	Unlike NREM where delta is a marker of *reduced* mean firing rate (lots of DOWN states), delta in wake arises from neuronal network dysregulation, not reduced net synaptic drive → **increased production.**
	EEG Theta Power	Marker of engaged wakefulness (navigation, memory tasks, active exploration); most prominent in the hippocampus and medial temporal cortex.	**None expected.**	Reflects highly organized excitatory synaptic activity; net synaptic firing is high → **increased production**
	EEG Beta Power	During wake indicates active, sustained cortical processing in distributed pyramidal–interneuron loops.	**None expected.**	Beta-associated states involve sustained, structured excitatory input → **increased production.**

Data availability

The data supporting the results in this study are available from the corresponding author with Institutional Review Board approval and Data Use Agreement permitting non-commercial use of data for independent validation, publication and sharing of new findings. For participants with one or more measures that failed the pipeline processing quality control, we will, upon special request, provide the measures that passed quality control, along with the unprocessed sensor data for the others where possible.

Code availability

Code used for the analysis and to produce the figures will be available on Zenodo. The code for the compartment model simulations is available on github.com[75].

FIGURES

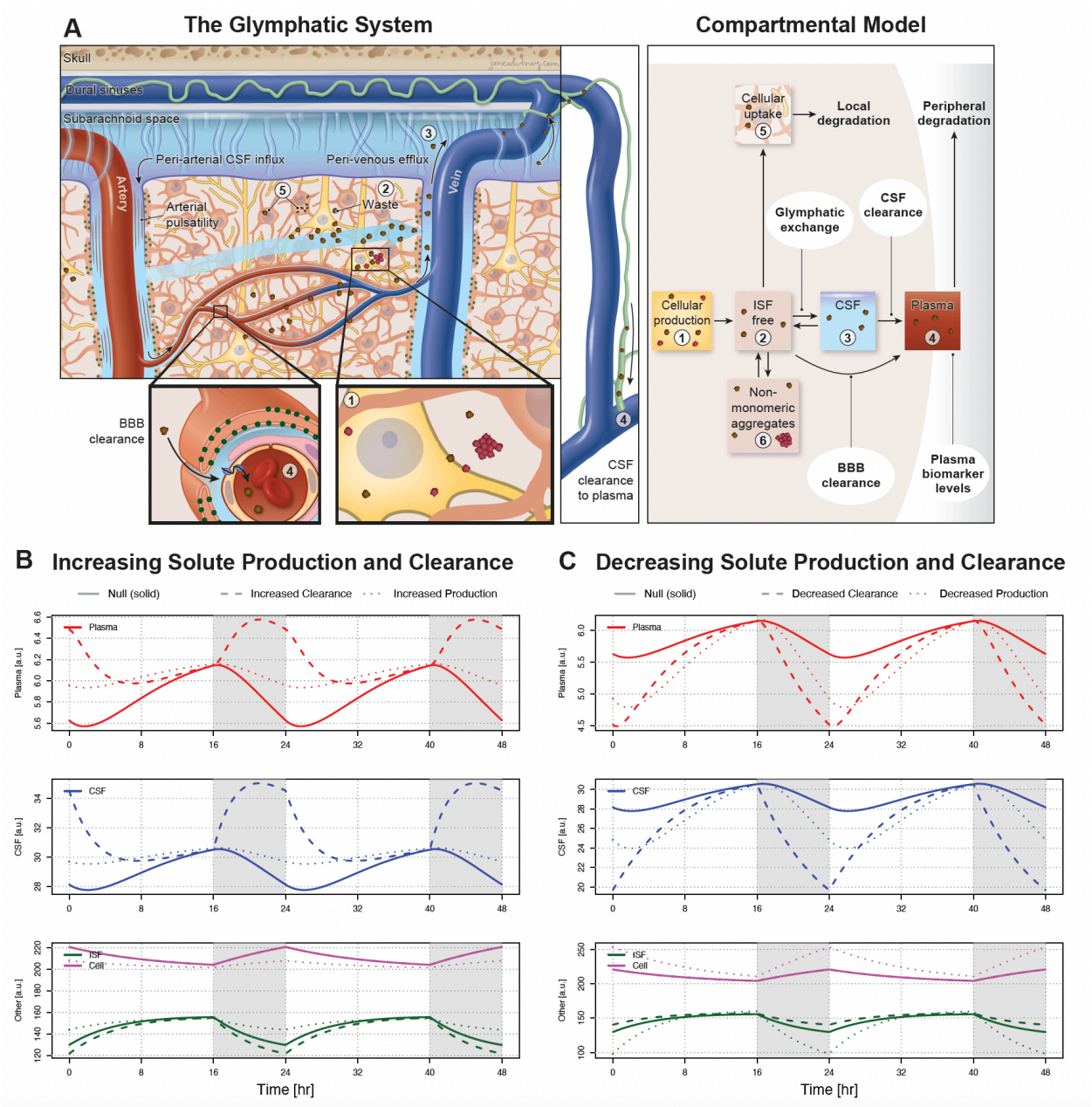

Figure 1. Six-compartment model of brain to plasma solute exchange.

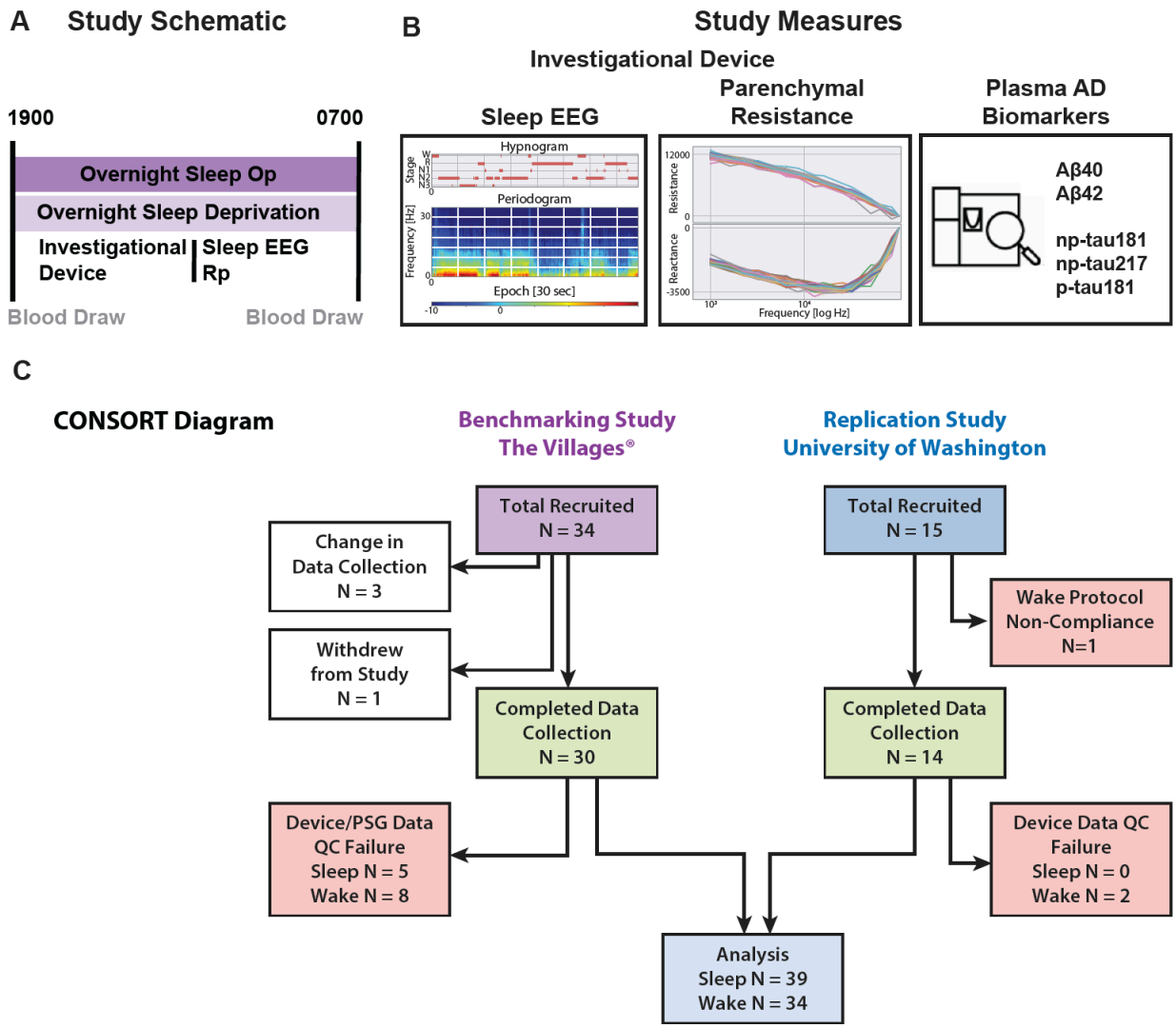

Figure 2. Study schematic and CONSORT diagram.

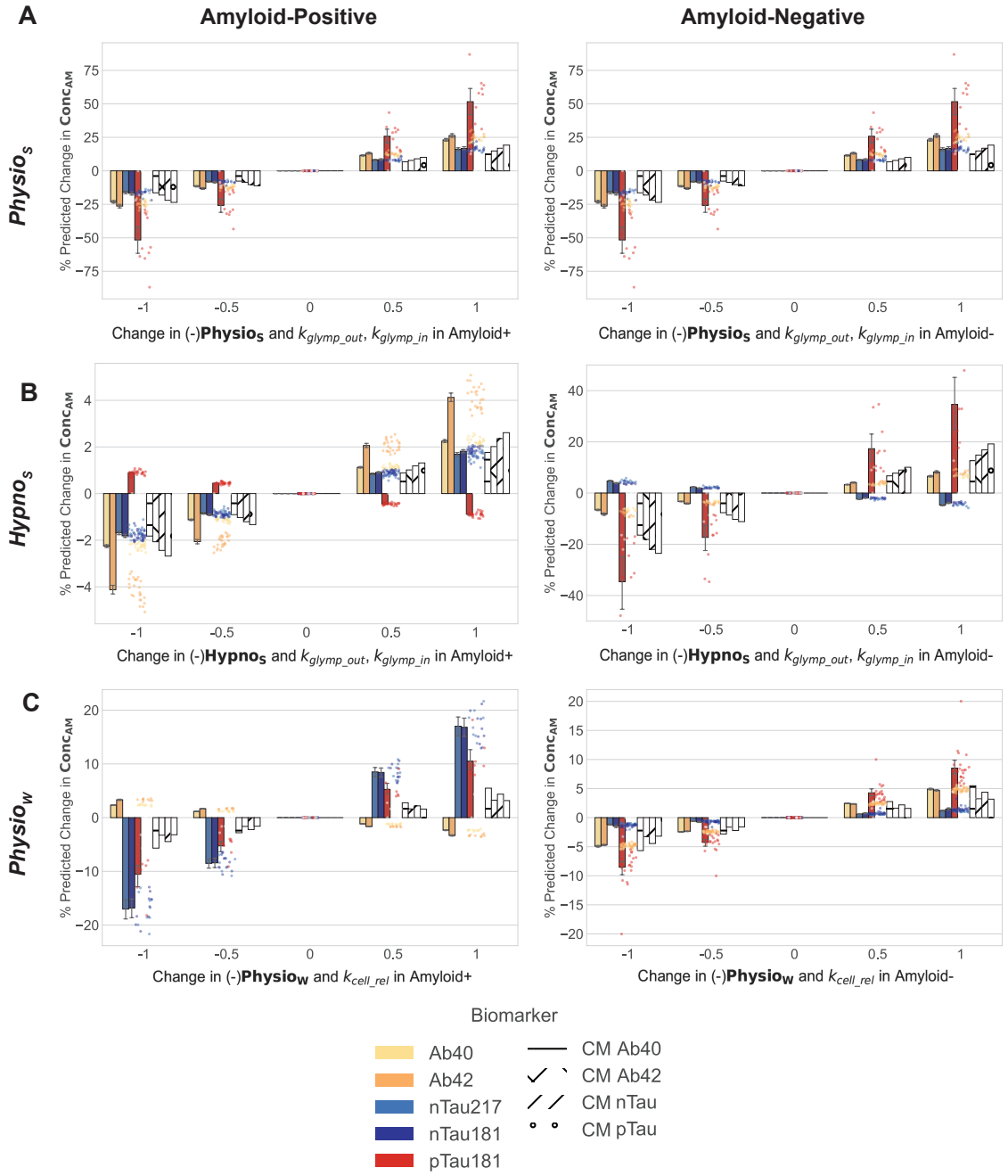

Figure 3. Comparison of neuro-glymphatic model and multicompartment model predictions of morning plasma AD biomarker levels.

TABLES

Table 1: Compartment rate constants of amyloid β and tau transport*

Rate Constant	Compartments	Process	Aβ Value	Tau Value
k_{cell_rel}	1 → 2	Cell solute production and release	$0.1\ hr^{-1}$	$0.1\ hr^{-1}$
k_{glymph_out}	2 → 3	Glymphatic interstitial solute efflux	$0.151\ hr^{-1}$	$0.151\ hr^{-1}$
k_{glymph_in}	3 → 2	Glymphatic CSF solute influx	$0.151\ hr^{-1}$	$0.151\ hr^{-1}$
k_{24}	2 → 4	Blood-brain barrier solute efflux	$0.1 \times 0.1\ hr^{-1}$	0
k_{25}	2 → 5	Local cellular uptake and degradation within the neuropil	$0.1 \times 0.9\ hr^{-1}$	$0.1 \times 0.9\ hr^{-1}$
k_{34}	3 → 4	CSF clearance	$0.151\ hr^{-1}$	$0.151\ hr^{-1}$
k_{4e}	4 → *elimination*	Peripheral elimination	$1.0\ hr^{-1}$	$1.0\ hr^{-1}$
k_{5e}	5 → *elimination*	Local cellular degradation	$1.0\ hr^{-1}$	$1.0\ hr^{-1}$
$k_{on-rate}$	2 → 6	Conversion rate from monomer to non-monomeric forms in ISF†	$7.2\ hr^{-1}$	$7.2\ hr^{-1}$
$k_{off-rate}$	6 → 2	Conversion rate from non-monomer to monomeric forms in ISF†	$0.32\ hr^{-1}$	$0.32\ hr^{-1}$

*Published rate constants[27,28].

†These values are for Aβ42 and p-tau. Values for Aβ40 and np-tau are 0.

Table 2. Clinical study demographic information*

Study	Age	Sex (F/M)	APOE-e4 (+/-)	Amyloid Plaque Status (+/-)	MoCA	GDS
Villages	61.9 (2.7)	13/12	7/18	11/14	27.9 (1.2)	0.7 (1.2)
University of Washington	55.9 (4.6)	6/7	4/9	0/13	28.5 (1.2)	0.5 (1.1)
Combined	59.8 (4.5)	19/19	11/27	11/27	28.1 (1.2)	0.7 (1.2)

*Values are Mean (SD) or count. MoCA, Montreal Cognitive Assessment; GDS, Geriatric Depression Scale. Amyloid plaque status determined using C_2N PrecivityAD test with cutoff of 0.089[32,34,35].

Table 3. Morning and evening plasma AD biomarker levels in sleep and sleep deprivation conditions.

Condition	Amyloid Status	Plasma Biomarker [units]	Morning Plasma Levels (*Conc*$_{AM}$)	Evening Plasma Levels (*Conc*$_{PM}$)	Differences (evening – morning)	DF	P (evening v morning)	P (sleep v wake)
Sleep	Positive	$A\beta_{40}$ [pg/mL]	401.8 (56.8)	412.5 (72.6)	10.71 (37.9)	10	0.371	0.682
		$A\beta_{42}$ [pg/mL]	32.2 (5.6)	33.2 (6.2)	1.05 (4.01)	10	0.406	0.895
		np-tau181 [pg/mL]	89.8 (20.8)	92.7 (23.2)	2.87 (10.9)	10	0.401	0.118
		np-tau217 [pg/mL]	101.3 (25.3)	108.3 (25.7)	7.05 (16.2)	10	0.179	0.210
		p-tau181 [pg/mL]	13.2 (4.7)	14.4 (5.7)	1.26 (1.7)	10	**0.035**	0.102
	Negative	Ab_{40} [pg/mL]	411.6 (55.4)	423.8 (50.5)	12.18 (25.7)	24	**0.026**	0.998
		Ab_{42} [pg/mL]	42.4 (5.8)	45.4 (5.8)	2.94 (4.96)	24	**0.007**	0.235
		np-tau181 [pg/mL]	66.8 (19.3)	68.5 (29.4)	1.70 (15.5)	26	0.574	0.218
		np-tau217 [pg/mL]	83.2 (24.2)	84.9 (35.3)	1.68 (20.4)	26	0.673	0.088
		p-tau181 [pg/mL]	9.5 (3.0)	10.2 (4.0)	0.68 (2.22)	26	0.122	0.791
Sleep Deprivation / Wake	Positive	$A\beta_{40}$ [pg/mL]	426.8 (69.8)	431.4 (72.2)	4.52 (28.6)	8	0.648	
		$A\beta_{42}$ [pg/mL]	35.1 (5.8)	36.4 (5.4)	1.26 (2.95)	8	0.237	
		np-tau181 [pg/mL]	84.7 (18.0)	100.4 (34.9)	15.64 (20.5)	8	0.051	
		np-tau217 [pg/mL]	97.0 (23.0)	116.2 (42.5)	19.20 (23.6)	8	**0.040**	
		p-tau181 [pg/mL]	13.8 (5.2)	16.6 (6.3)	2.80 (2.15)	8	**0.005**	
	Negative	$A\beta_{40}$ [pg/mL]	379.4 (35.2)	391.6 (43.8)	12.16 (33.7)	22	0.098	
		$A\beta_{42}$ [pg/mL]	39.6 (4.7)	41.1 (5.5)	1.56 (2.78)	22	**0.013**	
		np-tau181 [pg/mL]	57.1 (19.3)	63.8 (25.6)	6.69 (12.8)	22	**0.020**	
		np-tau217 [pg/mL]	68.6 (21.4)	79.2 (30.8)	10.59 (15.7)	22	**0.004**	
		p-tau181 [pg/mL]	8.1 (2.6)	9.0 (3.0)	0.85 (2.12)	22	0.069	

*Data shown as mean (SD). ***Conc***$_{AM}$, morning plasma level; ***Conc***$_{PM}$, evening plasma level; DF, degrees of freedom; **Bolded P values reflect significant associations at P < 0.05 using a paired two-tailed Student's t-test of significance.** First column of P values (evening v morning) tests evening versus morning biomarker plasma level differences. Second column of P values (sleep v wake) tests sleep versus wake change in evening-morning differences of biomarker plasma levels.

Table 4. Full model predictors and optimal weights predicting morning plasma AD biomarker levels in sleep and sleep deprivation conditions .

Condition and Predictor	Amyloid Status	Predictors	Estimate	CI	Wald's P
Sleep Condition ***Physio$_S$***	**Positive**	**R_p**	**0.968**	**0.177 – 0.998**	**0.036**
		PTT (NREM)	-0.034	-0.396 – 0.132	0.388
		HRV (NREM)	**-0.068**	**-0.464 – -0.014**	**0.030**
		EEG Delta Power (NREM)	0.086	-0.198 – 0.705	0.399
		EEG Theta Power (NREM)	0.162	-0.261 – 0.604	0.195
		EEG Theta Power (REM)	-0.146	-0.547 – 0.496	0.436
		EEG Beta Power (REM)	-0.041	-0.671 – 0.095	0.264
	Negative	**R_p**	**0.963**	**0.948 – 0.977**	**<0.001**
		PTT (NREM)	**-0.058**	**-0.200 – -0.028**	**0.006**
		HRV (NREM)	0.114	-0.003 – 0.178	0.060
		EEG Delta Power (NREM)	**-0.041**	**-0.149 – -0.010**	**0.026**
		EEG Theta Power (NREM)	**0.169**	**0.083 – 0.218**	**<0.001**
		EEG Theta Power (REM)	**0.087**	**0.001 – 0.133**	**0.058**
		EEG Beta Power (REM)	**-0.135**	**-0.250 – -0.093**	**<0.001**
Sleep Condition ***Hypnos$_S$***	**Positive**	NREM Duration	-0.182	-0.629 – 0.108	0.166
		REM Duration	-0.519	-0.829 – 0.337	0.209
		N1 Duration	**0.834**	**0.366 – 0.990**	**0.010**
		WASO Duration	0.044	-0.396 – 0.477	0.620
	Negative	**NREM Duration**	**-0.090**	**-0.239 – -0.054**	**0.001**
		REM Duration	**0.525**	**0.423 – 0.585**	**<0.001**
		N1 Duration	**0.801**	**0.754 – 0.855**	**<0.001**
		WASO Duration	**0.273**	**0.131 – 0.344**	**0.019**
Sleep Deprivation/Wake ***Physio$_W$***	**Positive**	R_p	0.621	-0.365 – 0.891	0.087
		PTT	0.190	-0.134 – 0.505	0.390
		HRV	-0.242	-0.450 – 0.106	0.166
		EEG Delta Power	**-0.487**	**-0.831 – -0.124**	**0.027**
		EEG Theta Power	-0.382	-0.670 – 0.584	0.339
		EEG Beta Power	0.371	-0.036 – 0.690	0.071
	Negative	**R_p**	**0.626**	**0.519 – 0.651**	**<0.001**
		PTT	-0.004	-0.127 – 0.029	0.461
		HRV	**0.136**	**0.058 – 0.173**	**0.028**
		EEG Delta Power	**-0.658**	**-0.717 – -0.634**	**<0.001**
		EEG Theta Power	**-0.391**	**-0.473 – -0.359**	**<0.001**
		EEG Beta Power	0.062	-0.026 – 0.095	0.170

*CI, 95% Confidence Interval; R_p, Parenchymal Resistance; PTT, Pulse Transit Time; HRV, Heart Rate Variability; EEG, Electroencephalography; ***Physio$_S$*** and ***Physio$_W$***, single predictors constructed from the linear combination of the full model predictors during the sleep and sleep deprivation (wake) conditions, respectively, for both amyloid positive and negative participants separately; ***Hypnos$_S$***, single predictor constructed from the full model hypnogram features during the sleep condition for both amyloid positive and negative participants separately. The estimated weights were selected using optimization to maximize the log likelihood of the production/clearance model. **Bolded P values reflect significant associations at P < 0.05 using bias-corrected bootstrapping.**

Table 5: Prediction of morning plasma AD biomarker levels following overnight sleep using the *null model* and the *neuro-glymphatic model* with *Physio$_S$*.

Model	Predictor Group	Predictor		Amyloid Positive				Amyloid Negative			
				Estimate	DF	CI	P	Estimate	DF	CI	P
Null Model	Fixed Effects	Age		-0.827	42	-1.856 – 0.203	0.113	0.075	108	-0.074 – 0.223	0.323
		Sex (male)		4.504	42	0.026 – 8.982	**0.049**	0.652	108	-0.587 – 1.890	0.299
		APOE-ε4 (positive)		-2.148	42	-6.949 – 2.652	0.372	-1.077	108	-2.365 – 0.212	0.101
		Circadian		0.039	42	-0.055 – 0.133	0.411	0.003	108	-0.008 – 0.014	0.590
		Study (Villages)		-	-	-	-	-1.309	108	-2.986 – 0.367	0.124
		Evening Biomarker Effects	***Conc$_{PM}$***	0.929	42	0.882 – 0.976	**<0.001**	0.959	108	0.933 – 0.986	**<0.001**
	Random Effects	σ^2		37.327				3.842			
		$\tau_{11\ pid\ Ab40}$		1.398				0.000			
		$\tau_{11\ pid\ Ab42}$		1.289				18.558			
		$\tau_{11\ Aggregate}$	$\tau_{11\ pid\ np\text{-}tau181}$	34.643				193.466			
			$\tau_{11\ pid\ np\text{-}tau217}$					352.682			
			$\tau_{11\ pid\ p\text{-}tau181}$					1.482			
Neuro-Glymphatic Model	Fixed Effects	Age		2.992	36	1.552 – 4.431	**<0.001**	0.137	98	0.050 – 0.224	**0.002**
		Sex (male)		-5.951	36	-10.868 – -1.034	**0.019**	0.768	98	0.057 – 1.479	**0.034**
		APOE-ε4 (positive)		-6.993	36	-9.946 – -4.039	**<0.001**	-0.580	98	-1.314 – 0.154	0.120
		Circadian		-0.158	36	-0.236 – -0.079	**<0.001**	0.008	98	0.002 – 0.015	**0.010**
		Study (Villages)		-	-	-	-	0.274	98	-0.831 – 1.379	0.623
		Evening Biomarker Effects	***Conc$_{PM}$***	4.067	36	3.129 – 5.004	**<0.001**	1.043	98	0.919 – 1.167	**<0.001**
		Predictor Effects	Aβ40: ***Physio$_S$***	-150.535	36	-290.48 – -10.586	**0.036**	5.190	98	-2.328 – 12.71	0.174
			Aβ42: ***Physio$_S$***	-152.504	36	-290.41 – -14.597	**0.031**	20.988	98	9.22 – 32.758	**0.001**
			np-tau181: ***Physio$_S$***	-173.692	36	-312.086 – -35.298	**0.015**	31.638	98	23.24 – 40.04	**<0.001**
			np-tau217: ***Physio$_S$***		36			44.178	98	31.69 – 56.67	**<0.001**
			p-tau181: ***Physio$_S$***		36			1.760	98	-0.935 – 4.456	0.198
		Evening Biomarker: Predictor Interactions	(Aβ40: ***Physio$_S$***) ***Conc$_{PM}$***	-4.284	36	-5.550 – -3.018	**<0.001**	-0.258	98	-0.46 – -0.055	**0.013**
			(Aβ42: ***Physio$_S$***) ***Conc$_{PM}$***	-4.371	36	-5.678 – -3.064	**<0.001**	-0.631	98	-0.91 – -0.353	**<0.001**
			(np-tau181:***Physio$_S$***) ***Conc$_{PM}$***	-3.742	36	-4.862 – -2.621	**<0.001**	-0.559	98	-0.72 – -0.399	**<0.001**
			np-tau217 ***Physio$_S$***) ***Conc$_{PM}$***					-0.605	98	-0.78 – -0.430	**<0.001**
			(p-tau181: ***Physio$_S$***) ***Conc$_{PM}$***					-0.528	98	-0.71 – -0.351	**<0.001**
	Random Effects	σ^2		17.538				0.608			
		$\tau_{11\ pid\ Ab40}$		12.406				6.374			
		$\tau_{11\ pid\ Ab42}$		12.432				19.957			
		$\tau_{11\ Aggregate}$	$\tau_{11\ pid\ np\text{-}tau181}$	2.105				71.422			
			$\tau_{11\ pid\ np\text{-}tau217}$					157.855			
			$\tau_{11\ pid\ p\text{-}tau181}$					0.345			

*DF, degrees of freedom; CI, 95% confidence interval; P, p-value; ***Physio$_S$***, single predictor constructed from the linear combination of parenchymal resistance R_P, cardio/cerebrovascular metrics and EEG powerbands; ***Conc$_{PM}$***, evening plasma level; UF, University of Florida study site; EEG, Electroencephalography; R_P, Parenchymal Resistance; σ^2, residual variance; τ_{11}, random slope variance; **Bolded P values reflect significant associations at P < 0.05**. Shaded cells demark random effects and potential biological confounders

Table 6: Likelihood ratio test of the *neuro-glymphatic model* versus the *null model.**

Condition and Predictor	Amyloid Status	Model	AIC	BIC	logLik	LRT	DF	P
Sleep Condition, *Physio$_S$*	**Positive**	Null	396.0	422.1	-185.0			
		Model	362.9	401.0	-162.4	45.2	6	**<0.001**
	Negative	Null	814.5	880.6	-384.2			
		Model	735.4	830.2	-334.7	99.1	10	**<0.001**
Sleep Condition, *Hypno$_S$*	**Positive**	Null	396.0	422.1	-185.0			
		Model	381.4	419.5	-171.7	26.6	6	**<0.001**
	Negative	Null	814.5	880.6	-384.2			
		Model	741.6	836.5	-337.8	92.9	10	**<0.001**
Sleep Deprivation/Wake *Physio$_W$*	**Positive**	Null	337.4	360.9	-155.7			
		Model	281.0	315.3	-121.5	68.4	6	**<0.001**
	Negative	Null	688.6	751.8	-321.3			
		Model	623.5	714.1	-278.8	85.1	10	**<0.001**

*AIC, Akaike Information Criteria; BIC, Bayesian Information Criteria; logLik, log likelihood; LRT, log likelihood ratio; DF, degrees of freedom; P, p-value; ***Physio$_S$*** and ***Physio$_W$***, single predictors constructed from the linear combination of the full model predictors during the sleep and sleep deprivation (wake) conditions, respectively, for both amyloid positive and negative participants separately; ***Hypno$_S$***, single predictor constructed from the full model hypnogram features during the sleep condition for both amyloid positive and negative participants separately; **Bolded P values reflect significant LRT at P < 0.05**.

Table 7. Percent of variance in morning plasma AD biomarker levels explained by the *neuro-glymphatic model* over the *null model.**

Condition and Predictor	Amyloid Status	Plasma Biomarker	Variance Explained	CI
Sleep Condition *Physio$_S$*	**Positive**	All Biomarkers	**51.9%**	**38.6% – 84.3%**
		Ab40	**49.1%**	**22.4% – 92.8%**
		Ab42	**56.0%**	**5.4% – 91.4%**
		All Tau	**51.7%**	**35.6% – 83.7%**
	Negative	All Biomarkers	**91.1%**	**47.4% – 98.1%**
		Ab40	**97.8%**	**45.5% – 99.6%**
		Ab42	**93.7%**	**40.7% – 99.3%**
		np-tau217	**95.4%**	**42.9% – 99.3%**
		np-tau181	**94.1%**	**38.7% – 99.1%**
		p-tau181	**71.3%**	**49.0% – 97.3%**
Sleep Condition *Hypno$_S$*	**Positive**	All Biomarkers	**42.0%**	**32.5% – 81.8%**
		Ab40	**57.7%**	**16.1% – 91.4%**
		Ab42	**62.5%**	**9.1% – 90.8%**
		All Tau	**38.4%**	**28.9% – 80.7%**
	Negative	All Biomarkers	**87.4%**	**17.7% – 96.9%**
		Ab40	95.7%	-30.1% – 98.3%
		Ab42	87.1%	-39.7% – 97.2%
		np-tau217	**93.1%**	**21.4% – 98.6%**
		np-tau181	**90.9%**	**1.5% – 98.4%**
		p-tau181	**64.0%**	**26.4% – 96.8%**
Sleep Deprivation/Wake *Physio$_W$*	**Positive**	All Biomarkers	**68.9%**	**65.5% – 92.5%**
		Ab40	76.6%	-7.9% – 94.1%
		Ab42	-53.8%	-13.7% – 95.4%
		All Tau	**72.8%**	**68.0% – 92.7%**
	Negative	All Biomarkers	**85.1%**	**34.9% – 98.0%**
		Ab40	**92.5%**	**40.2% – 99.4%**
		Ab42	**93.3%**	**44.7% – 99.5%**
		np-tau217	60.7%	-184.8% – 95.9%
		np-tau181	84.3%	-44.6% – 98.7%
		p-tau181	**73.8%**	**34.9% 96.8%**

*CI, 95% confidence interval; P, p-value; ***Physio$_S$*** and ***Physio$_W$***, single predictors constructed from the linear combination of the full model predictors during the sleep and sleep deprivation (wake) conditions, respectively, for both amyloid positive and negative participants separately; ***Hypno$_S$***, single predictor constructed from the full model hypnogram features during the sleep condition for both amyloid positive and negative participants separately. **Bolded P values reflect significant values at P < 0.05**.

Table 8. Analysis of deviance using Type III Wald Chi-square test for *neuro-glymphatic model* interaction effects*.

Condition and Predictor	Amyloid Status		Chi-squared	DF	P
Sleep Condition *Physio$_S$*	**Positive**	Age	17.77	1	**<0.001**
		Sex (male)	6.02	1	**0.014**
		APOE-ε4 (positive)	23.06	1	**<0.001**
		Circadian	16.65	1	**<0.001**
		Conc$_{PM}$	77.38	1	**<0.001**
		Biomarker: ***Physio$_S$***	11.41	3	**0.010**
		Biomarker: ***Physio$_S$:Conc$_{PM}$***	50.81	3	**<0.001**
	Negative	Age	9.83	1	**0.002**
		Sex (male)	4.60	1	**0.032**
		APOE-ε4 (positive)	2.46	1	0.117
		Circadian	6.95	1	**0.008**
		Study (Villages)	0.24	1	0.622
		Conc$_{PM}$	279.80	1	**<0.001**
		Biomarker: ***Physio$_S$***	71.58	5	**<0.001**
		Biomarker: ***Physio$_S$:Conc$_{PM}$***	64.33	5	**<0.001**
Sleep Condition *Hypno$_S$*	**Positive**	Age	6.08	1	**0.014**
		Sex (male)	3.36	1	0.067
		APOE-ε4 (positive)	1.70	1	0.193
		Circadian	0.71	1	0.401
		Conc$_{PM}$	1226.73	1	**<0.001**
		Biomarker: ***Hypno$_S$***	10.98	3	**0.012**
		Biomarker: ***Hypno$_S$:Conc$_{PM}$***	32.27	3	**<0.001**
	Negative	Age	11.58	1	**0.001**
		Sex (male)	3.07	1	**0.080**
		APOE-ε4 (positive)	0.90	1	0.343
		Circadian	2.02	1	0.155
		Study (Villages)	0.97	1	0.325
		Conc$_{PM}$	906.49	1	**<0.001**
		Biomarker: ***Hypno$_S$***	117.52	5	**<0.001**
		Biomarker: ***Hypno$_S$:Conc$_{PM}$***	124.69	5	**<0.001**
Sleep deprivation/Wake *Physio$_W$*	**Positive**	Age	7.95	1	**0.005**
		Sex (male)	3.41	1	0.065
		APOE-ε4 (positive)	5.21	1	**0.022**
		Circadian	1.91	1	0.167
		Conc$_{PM}$	1758.09	1	**<0.001**
		Biomarker: ***Physio$_W$***	2.44	3	0.487
		Biomarker: ***Physio$_W$:Conc$_{PM}$***	95	3	**<0.001**
	Negative	Age	2.07	1	0.15
		Sex (male)	0.31	1	0.577
		APOE-ε4 (positive)	6.95	1	**0.008**
		Circadian	0.89	1	0.344
		Study (Villages)	5.16	1	**0.023**
		Conc$_{PM}$	4639.5	1	**<0.001**
		Biomarker: ***Physio$_W$***	146.77	5	**<0.001**
		Biomarker: ***Physio$_W$:Conc$_{PM}$***	185.9	5	**<0.001**

*DF, degrees of freedom; P, p-value; ***Physio$_S$*** and ***Physio$_W$***, single predictors constructed from the linear combination of the full model predictors during the sleep and sleep deprivation (wake) conditions, respectively, for both amyloid positive and negative participants separately; ***Hypno$_S$***, single predictor constructed from the full model hypnogram features during the sleep condition for both amyloid positive and negative participants separately; ***Conc$_{PM}$***, evening plasma level; **Bolded P values reflect significant associations at P < 0.05**.

FIGURE LEGENDS

Figure 1. Six-compartment model of brain to plasma solute exchange. (A) Amyloid β (Aβ) and tau are produced in neurons (**1**) and released into the ISF compartment (**2**) where they are cleared from the ISF via local cellular uptake (**2 → 5**) and degradation, blood-brain barrier efflux (**2 → 4**), or glymphatic efflux to the CSF (**2 → 3**). Aβ42 and phosphorylated tau species are prone to non-monomeric aggregation, unlike Aβ40 and non-phosphorylated tau. Their monomeric forms can also be cleared from the ISF through further aggregation into non-monomeric structures (**2 → 6**). CSF solutes may recirculate back into the brain interstitium (**3 → 2**) or be cleared by CSF efflux pathways to the plasma (**3 → 4**) from whence peripheral degradation occurs. **(B) – (C)** Compartment concentrations of monomeric amyloid β and tau at steady state in the **null model** and the **neuro-glymphatic model** following changes in glymphatic efflux/influx or synaptic and metabolic release. Release of cellular Aβ and tau species from neurons (**1**) into the ISF (**2**) in the model is controlled by the cellular solute release rate constant k_{cell_rel} and was kept constant during the 16 hours of wake and was reduced by 30% during the 8 hours of sleep occurring in the shaded window between16 and 24 hours. Solid lines show compartment concentrations under the **null model**, with time-invariant release rate constant k_{cell_rel} and time-invariant exchange between the CSF (**3**) and ISF (**2**) compartments. Long dashed lines show change in compartment concentrations when glymphatic efflux/influx rate constants k_{glymph_out} and k_{glymph_in}, were increased by a factor of 1.5 **(B)** or decreased by a factor 0.5 **(C)** during the 8-hour sleep window. Dotted lines show change in compartment concentrations when synaptic and metabolic release rate constant k_{cell_rel} was increased by a factor of 1.25 **(B)** or decreased by a factor of 0.5 **(C)** during the 8-hour sleep window. Note that increasing (decreasing) either glymphatic efflux/influx or synaptic and metabolic release during sleep increases (decreases) morning plasma level of Aβ and tau species relative to the **null model**.

Figure 2. Study schematic and CONSORT diagram.

The Benchmarking Study conducted at The Villages® and the Replication study conducted at the University of Washington were **(A)** randomized cross-over assignment of overnight sleep opportunity and overnight sleep deprivation designed to define the relationship between parenchymal resistance (R_P) and glymphatic function. **(B)** Reported here are the overnight investigational device recordings of R_P, EEG and HR, and blood analysis of amyloid β and tau levels (Aβ40, Aβ42, np-tau181, np-tau217 and p-tau181). **(C)** The Benchmarking Study enrolled 34 participants of which 30 completed both visits. Three were censored due to changes in device data collection and sensor locations. One withdrew following the first MRI scan. Of the 30 that completed the study, 5 overnight sleep visits and 8 overnight wake visits failed the data quality control (QC) criteria to provide sufficient artifact free data to yield results. This resulted in 25 sleep and 22 wake complete data sets. The Replication Study enrolled 14 participants. All 14 completed the study, of which 3 wake visits failed the data QC criteria and one sleep visit failed specific to the analysis of these data because of missing EEG powerband data during REM sleep caused by artifacts. The remaining 13 participants had complete data for analysis.

Figure 3. Comparison of neuro-glymphatic model and multicompartment model predictions of morning plasma level. The percent change prediction in morning plasma level $\boldsymbol{Conc_{AM}}$ of AD biomarkers $A\beta_{40}$, $A\beta_{42}$, np-tau181, np-tau217, p-tau181 resulting from a change in units of SD of the single predictors $\boldsymbol{Physio_S}$ **(A)**, $\boldsymbol{Hypno_S}$ **(B)**, and $\boldsymbol{Physio_W}$ **(C)** of the **neuro-glymphatic model** in amyloid-positive and amyloid-negative participants are compared against

the percent change in the morning amyloid β and tau multicompartment model prediction from a corresponding change glymphatic efflux/influx rate constants k_{glymph_out} and k_{glymph_in} **(A)** and **(B)**, or synaptic and metabolic release rate constant k_{cell_rel} **(C)**. Predicted mean and 95% confidence intervals for $A\beta_{40}$, $A\beta_{42}$, np-tau181, np-tau217, p-tau181 at each SD change in the single predictor are shown in order as the first five bars alongside the **neuro-glymphatic model** predictions for that SD change. Multicompartment model predictions for $A\beta 40$, $A\beta 42$, non-phosphorylated and phosphorylated tau at each corresponding change of the rate constants k_{glymph_out} and k_{glymph_in} **(A)** and **(B)**, or k_{cell_rel} **(C)**, are shown in order as the last four hatched bars. The change in the negative of the single predictors are shown for comparison with the change in the rate constants. For example, a 1SD increase in the negative predictor corresponds to a 1SD decrease in the actual predictor.

REFERENCES

1 Robbins, R. *et al.* Examining sleep deficiency and disturbance and their risk for incident dementia and all-cause mortality in older adults across 5 years in the United States. *Aging (Albany NY)* **13**, 3254-3268 (2021). https://doi.org/10.18632/aging.202591

2 Lutsey, P. L. *et al.* Sleep characteristics and risk of dementia and Alzheimer's disease: The Atherosclerosis Risk in Communities Study. *Alzheimers Dement* **14**, 157-166 (2018). https://doi.org/10.1016/j.jalz.2017.06.2269

3 Lim, A. S., Kowgier, M., Yu, L., Buchman, A. S. & Bennett, D. A. Sleep Fragmentation and the Risk of Incident Alzheimer's Disease and Cognitive Decline in Older Persons. *Sleep* **36**, 1027-1032 (2013). https://doi.org/10.5665/sleep.2802

4 Liu, H. *et al.* Acute sleep loss decreases CSF-to-blood clearance of Alzheimer's disease biomarkers. *Alzheimers Dement* (2023). https://doi.org/10.1002/alz.12930

5 Sprecher, K. E. *et al.* Poor sleep is associated with CSF biomarkers of amyloid pathology in cognitively normal adults. *Neurology* **89**, 445-453 (2017). https://doi.org/10.1212/WNL.0000000000004171

6 Sprecher, K. E. *et al.* Amyloid burden is associated with self-reported sleep in nondemented late middle-aged adults. *Neurobiol Aging* **36**, 2568-2576 (2015). https://doi.org/10.1016/j.neurobiolaging.2015.05.004

7 Spira, A. P. *et al.* Self-reported sleep and β-amyloid deposition in community-dwelling older adults. *JAMA Neurol* **70**, 1537-1543 (2013). https://doi.org/10.1001/jamaneurol.2013.4258

8 Winer, J. R. *et al.* Association of Short and Long Sleep Duration With Amyloid-β Burden and Cognition in Aging. *JAMA Neurol* **78**, 1187-1196 (2021). https://doi.org/10.1001/jamaneurol.2021.2876

9 Insel, P. S., Mohlenhoff, B. S., Neylan, T. C., Krystal, A. D. & Mackin, R. S. Association of Sleep and β-Amyloid Pathology Among Older Cognitively Unimpaired Adults. *JAMA Netw Open* **4**, e2117573 (2021). https://doi.org/10.1001/jamanetworkopen.2021.17573

10 Iliff, J. J. *et al.* A paravascular pathway facilitates CSF flow through the brain parenchyma and the clearance of interstitial solutes, including amyloid β. *Sci Transl Med* **4**, 147ra111 (2012). https://doi.org/10.1126/scitranslmed.3003748

11 Iliff, J. J. *et al.* Brain-wide pathway for waste clearance captured by contrast-enhanced MRI. *J Clin Invest* **123**, 1299-1309 (2013). https://doi.org/10.1172/JCI67677

12 Iliff, J. J. *et al.* Cerebral arterial pulsation drives paravascular CSF-interstitial fluid exchange in the murine brain. *J Neurosci* **33**, 18190-18199 (2013). https://doi.org/10.1523/JNEUROSCI.1592-13.2013

13 Xie, L. *et al.* Sleep drives metabolite clearance from the adult brain. *Science* **342**, 373-377 (2013). https://doi.org/10.1126/science.1241224

14 Iliff, J. J. *et al.* Impairment of glymphatic pathway function promotes tau pathology after traumatic brain injury. *J Neurosci* **34**, 16180-16193 (2014). https://doi.org/10.1523/JNEUROSCI.3020-14.2014

15 Harrison, I. F. *et al.* Impaired glymphatic function and clearance of tau in an Alzheimer's disease model. *Brain* **143**, 2576-2593 (2020). https://doi.org/10.1093/brain/awaa179

16 Eide, P. K., Vinje, V., Pripp, A. H., Mardal, K. A. & Ringstad, G. Sleep deprivation impairs molecular clearance from the human brain. *Brain* **144**, 863-874 (2021). https://doi.org/10.1093/brain/awaa443

17 Dagum, P. *et al.* A wireless device for continuous measurement of brain parenchymal resistance tracks glymphatic function in humans. *Nat Biomed Eng* (2025). https://doi.org/10.1038/s41551-025-01394-9
18 Blennow, K. *et al.* The potential clinical value of plasma biomarkers in Alzheimer's disease. *Alzheimers Dement* **19**, 5805-5816 (2023). https://doi.org/10.1002/alz.13455
19 Rissman, R. A. *et al.* Plasma Aβ42/Aβ40 and phospho-tau217 concentration ratios increase the accuracy of amyloid PET classification in preclinical Alzheimer's disease. *Alzheimers Dement* **20**, 1214-1224 (2024). https://doi.org/10.1002/alz.13542
20 Benedict, C., Blennow, K., Zetterberg, H. & Cedernaes, J. Effects of acute sleep loss on diurnal plasma dynamics of CNS health biomarkers in young men. *Neurology* **94**, e1181-e1189 (2020). https://doi.org/10.1212/WNL.0000000000008866
21 Eide, P. K. *et al.* Plasma neurodegeneration biomarker concentrations associate with glymphatic and meningeal lymphatic measures in neurological disorders. *Nat Commun* **14**, 2084 (2023). https://doi.org/10.1038/s41467-023-37685-5
22 Hablitz, L. M. *et al.* Increased glymphatic influx is correlated with high EEG delta power and low heart rate in mice under anesthesia. *Sci Adv* **5**, eaav5447 (2019). https://doi.org/10.1126/sciadv.aav5447
23 Jiang-Xie, L. F. *et al.* Neuronal dynamics direct cerebrospinal fluid perfusion and brain clearance. *Nature* **627**, 157-164 (2024). https://doi.org/10.1038/s41586-024-07108-6
24 Dagum, P. *et al.* The use of continuous brain parenchymal impedance dispersion to measure glymphaticfunction in humans. *medRxiv* (2024). https://doi.org/10.1101/2024.01.06.24300933
25 van Veluw, S. J. *et al.* Vasomotion as a Driving Force for Paravascular Clearance in the Awake Mouse Brain. *Neuron* **105**, 549-561.e545 (2020). https://doi.org/10.1016/j.neuron.2019.10.033
26 Fultz, N. E. *et al.* Coupled electrophysiological, hemodynamic, and cerebrospinal fluid oscillations in human sleep. *Science* **366**, 628-631 (2019). https://doi.org/10.1126/science.aax5440
27 Elbert, D. L., Patterson, B. W., Lucey, B. P., Benzinger, T. L. S. & Bateman, R. J. Importance of CSF-based Aβ clearance with age in humans increases with declining efficacy of blood-brain barrier/proteolytic pathways. *Commun Biol* **5**, 98 (2022). https://doi.org/10.1038/s42003-022-03037-0
28 Michaels, T. C. T. *et al.* Dynamics of oligomer populations formed during the aggregation of Alzheimer's Aβ42 peptide. *Nat Chem* **12**, 445-451 (2020). https://doi.org/10.1038/s41557-020-0452-1
29 Kang, J. E. *et al.* Amyloid-beta dynamics are regulated by orexin and the sleep-wake cycle. *Science* **326**, 1005-1007 (2009). https://doi.org/10.1126/science.1180962
30 Holth, J. K. *et al.* The sleep-wake cycle regulates brain interstitial fluid tau in mice and CSF tau in humans. *Science* **363**, 880-884 (2019). https://doi.org/10.1126/science.aav2546
31 Cirrito, J. R. *et al.* Synaptic activity regulates interstitial fluid amyloid-beta levels in vivo. *Neuron* **48**, 913-922 (2005). https://doi.org/10.1016/j.neuron.2005.10.028
32 Meyer, M. R. *et al.* Clinical validation of the PrecivityAD2 blood test: A mass spectrometry-based test with algorithm combining %p-tau217 and Aβ42/40 ratio to identify presence of brain amyloid. *Alzheimers Dement* **20**, 3179-3192 (2024). https://doi.org/10.1002/alz.13764

33 Fogelman, I. *et al.* Independent study demonstrates amyloid probability score accurately indicates amyloid pathology. *Ann Clin Transl Neurol* **10**, 765-778 (2023). https://doi.org/10.1002/acn3.51763
34 Hu, Y. *et al.* Assessment of a Plasma Amyloid Probability Score to Estimate Amyloid Positron Emission Tomography Findings Among Adults With Cognitive Impairment. *JAMA Netw Open* **5**, e228392 (2022). https://doi.org/10.1001/jamanetworkopen.2022.8392
35 West, T. *et al.* A blood-based diagnostic test incorporating plasma Aβ42/40 ratio, ApoE proteotype, and age accurately identifies brain amyloid status: findings from a multi cohort validity analysis. *Mol Neurodegener* **16**, 30 (2021). https://doi.org/10.1186/s13024-021-00451-6
36 Orduña Dolado, A. *et al.* Effects of time of the day at sampling on CSF and plasma levels of Alzheimer' disease biomarkers. *Alzheimers Res Ther* **16**, 132 (2024). https://doi.org/10.1186/s13195-024-01503-x
37 Du, L. *et al.* Longitudinal plasma phosphorylated-tau217 and other related biomarkers in a non-demented Alzheimer's risk-enhanced sample. *Alzheimers Dement* (2024). https://doi.org/10.1002/alz.14100
38 Barthélemy, N. R. *et al.* Highly accurate blood test for Alzheimer's disease is similar or superior to clinical cerebrospinal fluid tests. *Nat Med* **30**, 1085-1095 (2024). https://doi.org/10.1038/s41591-024-02869-z
39 Park, H., Tarpey, T., Petkova, E. & Ogden, R. T. A high-dimensional single-index regression for interactions between treatment and covariates. *Statistical Papers* (2024). https://doi.org/10.1007/s00362-024-01546-0
40 Mestre, H. *et al.* Flow of cerebrospinal fluid is driven by arterial pulsations and is reduced in hypertension. *Nat Commun* **9**, 4878 (2018). https://doi.org/10.1038/s41467-018-07318-3
41 Hauglund, N. L. *et al.* Norepinephrine-mediated slow vasomotion drives glymphatic clearance during sleep. *Cell* **188**, 606-622.e617 (2025). https://doi.org/10.1016/j.cell.2024.11.027
42 Jack, C. R. *et al.* NIA-AA Research Framework: Toward a biological definition of Alzheimer's disease. *Alzheimers Dement* **14**, 535-562 (2018). https://doi.org/10.1016/j.jalz.2018.02.018
43 Biel, D. *et al.* Tau-PET and in vivo Braak-staging as prognostic markers of future cognitive decline in cognitively normal to demented individuals. *Alzheimers Res Ther* **13**, 137 (2021). https://doi.org/10.1186/s13195-021-00880-x
44 Jack, C. R. *et al.* Revised criteria for diagnosis and staging of Alzheimer's disease: Alzheimer's Association Workgroup. *Alzheimers Dement* (2024). https://doi.org/10.1002/alz.13859
45 van Dyck, C. H. *et al.* Lecanemab in Early Alzheimer's Disease. *N Engl J Med* **388**, 9-21 (2023). https://doi.org/10.1056/NEJMoa2212948
46 Sims, J. R. *et al.* Donanemab in Early Symptomatic Alzheimer Disease: The TRAILBLAZER-ALZ 2 Randomized Clinical Trial. *JAMA* **330**, 512-527 (2023). https://doi.org/10.1001/jama.2023.13239
47 Mestre, H. *et al.* Aquaporin-4-dependent glymphatic solute transport in the rodent brain. *Elife* **7** (2018). https://doi.org/10.7554/eLife.40070

48 Pedersen, T. J., Keil, S. A., Han, W., Wang, M. X. & Iliff, J. J. The effect of aquaporin-4 mis-localization on Aβ deposition in mice. *Neurobiol Dis* **181**, 106100 (2023). https://doi.org/10.1016/j.nbd.2023.106100
49 Simon, M. *et al.* Loss of perivascular aquaporin-4 localization impairs glymphatic exchange and promotes amyloid β plaque formation in mice. *Alzheimers Res Ther* **14**, 59 (2022). https://doi.org/10.1186/s13195-022-00999-5
50 Xu, Z. *et al.* Deletion of aquaporin-4 in APP/PS1 mice exacerbates brain Aβ accumulation and memory deficits. *Mol Neurodegener* **10**, 58 (2015). https://doi.org/10.1186/s13024-015-0056-1
51 Ishida, K. *et al.* Glymphatic system clears extracellular tau and protects from tau aggregation and neurodegeneration. *J Exp Med* **219** (2022). https://doi.org/10.1084/jem.20211275
52 Kress, B. T. *et al.* Impairment of paravascular clearance pathways in the aging brain. *Ann Neurol* **76**, 845-861 (2014). https://doi.org/10.1002/ana.24271
53 Li, M. *et al.* Impaired Glymphatic Function and Pulsation Alterations in a Mouse Model of Vascular Cognitive Impairment. *Front Aging Neurosci* **13**, 788519 (2021). https://doi.org/10.3389/fnagi.2021.788519
54 Wang, M. *et al.* Focal Solute Trapping and Global Glymphatic Pathway Impairment in a Murine Model of Multiple Microinfarcts. *J Neurosci* **37**, 2870-2877 (2017). https://doi.org/10.1523/JNEUROSCI.2112-16.2017
55 Braun, M. *et al.* Macroscopic changes in aquaporin-4 underlie blast traumatic brain injury-related impairment in glymphatic function. *Brain* **147**, 2214-2229 (2024). https://doi.org/10.1093/brain/awae065
56 Christensen, J., Wright, D. K., Yamakawa, G. R., Shultz, S. R. & Mychasiuk, R. Repetitive Mild Traumatic Brain Injury Alters Glymphatic Clearance Rates in Limbic Structures of Adolescent Female Rats. *Sci Rep* **10**, 6254 (2020). https://doi.org/10.1038/s41598-020-63022-7
57 Plog, B. A. *et al.* Biomarkers of traumatic injury are transported from brain to blood via the glymphatic system. *J Neurosci* **35**, 518-526 (2015). https://doi.org/10.1523/JNEUROSCI.3742-14.2015
58 Deng, S. *et al.* Chronic sleep fragmentation impairs brain interstitial clearance in young wildtype mice. *J Cereb Blood Flow Metab*, 271678X241230188 (2024). https://doi.org/10.1177/0271678X241230188
59 Nedergaard, M. & Goldman, S. A. Glymphatic failure as a final common pathway to dementia. *Science* **370**, 50-56 (2020). https://doi.org/10.1126/science.abb8739
60 Keil, S. A., Jansson, D., Braun, M. & Iliff, J. J. Glymphatic dysfunction in Alzheimer's disease: A critical appraisal. *Science* **389**, eadv8269 (2025). https://doi.org/10.1126/science.adv8269
61 Ringstad, G., Vatnehol, S. A. S. & Eide, P. K. Glymphatic MRI in idiopathic normal pressure hydrocephalus. *Brain* **140**, 2691-2705 (2017). https://doi.org/10.1093/brain/awx191
62 Eide, P. K. & Ringstad, G. Functional analysis of the human perivascular subarachnoid space. *Nat Commun* **15**, 2001 (2024). https://doi.org/10.1038/s41467-024-46329-1
63 Kronmal, R. A. Spurious Correlation and the Fallacy of the Ratio Standard Revisited. *Journal of the Royal Statistical Society,* **156**, 379-392 (1993).
64 C_2N <https://c2n.com/>

65 Balaji, Ananta Narayanan, Andrea Ferlini, Fahim Kawsar, and Alessandro Montanari. "Stereo-bp: Non-invasive blood pressure sensing with earables." In *Proceedings of the 24th International Workshop on Mobile Computing Systems and Applications*, pp. 96-102. 2023.

66 Lin, Weili, Azim Celik, and Richard P. Paczynski. "Regional cerebral blood volume: a comparison of the dynamic imaging and the steady state methods." *Journal of Magnetic Resonance Imaging: An Official Journal of the International Society for Magnetic Resonance in Medicine* 9, no. 1 (1999): 44-52.

67 Xu, R. Measuring explained variation in linear mixed effects models. *Stat Med* **22**, 3527-3541 (2003). https://doi.org/10.1002/sim.1572

68 Heinze, G., Wallisch, C. & Dunkler, D. Variable selection - A review and recommendations for the practicing statistician. *Biom J* **60**, 431-449 (2018). https://doi.org/10.1002/bimj.201700067

69 Berridge, D. M. & Crouchley, R. *Multivariate Generalized Linear Mixed Models Using R*. (CRC Press, 2011).

70 Xu, R. Measuring explained variation in linear mixed effects models. *Stat Med* **22**, 3527-3541 (2003). https://doi.org/10.1002/sim.1572

71 Helakari, H. *et al.* Human NREM Sleep Promotes Brain-Wide Vasomotor and Respiratory Pulsations. *J Neurosci* **42**, 2503-2515 (2022). https://doi.org/10.1523/JNEUROSCI.0934-21.2022

72 Benveniste, H. *et al.* Anesthesia with Dexmedetomidine and Low-dose Isoflurane Increases Solute Transport via the Glymphatic Pathway in Rat Brain When Compared with High-dose Isoflurane. *Anesthesiology* **127**, 976-988 (2017). https://doi.org/10.1097/ALN.0000000000001888

73 Hussain, R. *et al.* Potentiating glymphatic drainage minimizes post-traumatic cerebral oedema. *Nature* **623**, 992-1000 (2023). https://doi.org/10.1038/s41586-023-06737-7

74 Lucey, B. P., Fagan, A. M., Holtzman, D. M., Morris, J. C. & Bateman, R. J. Diurnal oscillation of CSF Aβ and other AD biomarkers. *Mol Neurodegener* **12**, 36 (2017). https://doi.org/10.1186/s13024-017-0161-4

75 Dagum, P., Corbellini, A., Singh, T. Compartment model simulation. *Github.com,* (2025). https://github.com/appliedcognition/ac_compartment_model_simulation